Contrib Mineral Petrol (1999) 137: 267–287

Jon Cox · Mike Searle · Rolf Pedersen

The petrogenesis of leucogranitic dykes intruding the northern Semail ophiolite, United Arab Emirates: field relationships, geochemistry and Sr/Nd isotope systematics

Received: 17 December 1998 / Accepted: 19 July 1999

Abstract The Khawr Fakkan block of the Semail ophiolite (United Arab Emirates) exhibits a suite of 10–100 m scale metaluminous to peraluminous granitic intrusions, ranging from cordierite-andalusite-biotite monzogranites to garnet-tourmaline leucogranites, which intrude mantle sequence harzburgites and lower crustal sequence cumulate gabbros. Structural constraints suggest that the subduction of continental sedimentary material beneath the hot proto-ophiolite in an intra-oceanic arc environment led to granulite facies metamorphism at the subduction front and the generation of granitic melts which were emplaced up to the level of the ophiolite Moho. Compositions indicate the analysed granitoids were largely minimum melts that crystallised at variable a_{H_2O} and pressures of 3 to 5 kbar. The LILE (Sr, Rb and Ba) covariation modelling suggests that the granitoids formed largely by the dehydration melting of muscovite rich metasediments. Initial $^{87}Sr/^{86}Sr$ ratios of analysed dykes vary between 0.710 and 0.706 at initial ε_{Nd} values of between −6.3 and −0.5. Cogenetic units of a composite sill from Ra's Dadnah yield a Sm-Nd isochron age of 98.8 ± 9.5 Ma (MSWD = 1.18). Geochemical and isotopic characteristics of the analysed granitic intrusions indicate that the subducted continental material was derived from oceanic trench fill (Haybi complex) sediments, preserved as greenschist (Asimah area) to granulite facies (Bani Hamid area) ophiolitic metamorphic sole terranes. The Sr-Nd isotope systematics suggest that hybrid granitic melts were derived from pre-magmatic mixing of two contrasting subduction zone sources.

J. Cox (✉) · M. Searle
Department of Earth Sciences, Oxford University, Parks Rd, Oxford, OX1 3PR, UK

R. Pedersen
Department of Geology, University of Bergen, N-5007, Bergen, Norway

Editorial responsibility: J. Hoefs

Introduction

Ophiolite obduction processes commonly involve emplacement of a slab of oceanic crust and upper mantle onto passive continental margins (Coleman 1981; Nicolas 1989). The Semail ophiolite of SE Arabia (Fig. 1) is the largest and most extensively studied ophiolite in the world. It forms a well exposed thrust sheet ~700 km in length, 100 km wide, and 10–15 km thick in the United Arab Emirates (UAE) and Oman (e.g. Glennie et al. 1974; Coleman and Hopson 1981; Lippard et al. 1986). The ophiolite is of Cenomanian age and formed ~95 Ma ago (Tilton et al. 1981; Tippit et al. 1981). Following intra-oceanic thrusting, it was transported up to 400–500 km SW (Bechennec et al. 1988) over the Tethyan Hawasina basin and was emplaced onto the Permian–Mesozoic passive continental margin of the Arabian plate during the late Cretaceous. The ophiolite complex was undoubtedly formed at an oceanic spreading center within Tethys. Controversy exists as to whether it formed at a mid ocean ridge (MOR) (Coleman 1981; Boudier et al. 1985, 1988; Hacker 1991; Hacker et al. 1996) or a supra-subduction zone (SSZ) setting (Searle and Malpas 1980; Pearce et al. 1981; Lippard et al. 1986; Searle and Cox 1999). However, it is generally accepted that obduction related thrusts propagated structurally downwards, towards the Arabian shelf margin as the emplacement process progressed generally in a WSW–SW direction. The entire obduction process lasted ~23 Ma and was completed by the end of the Lower Maastrichtian (~72 Ma) when shallow-marine fossiliferous limestones were deposited unconformably over all allochthonous units (Glennie et al. 1974).

Cordierite-andalusite-biotite bearing and other granitoid dykes in the Khawr Fakkan block of the Semail ophiolite have been variously interpreted. Proposed models have invoked extreme crystal fractionation in the ophiolite late intrusive series, or (at least in part), partial melting of the metamorphic sole at the base of the ophiolite (Peters and Kamber 1994; Gnos and Nicolas

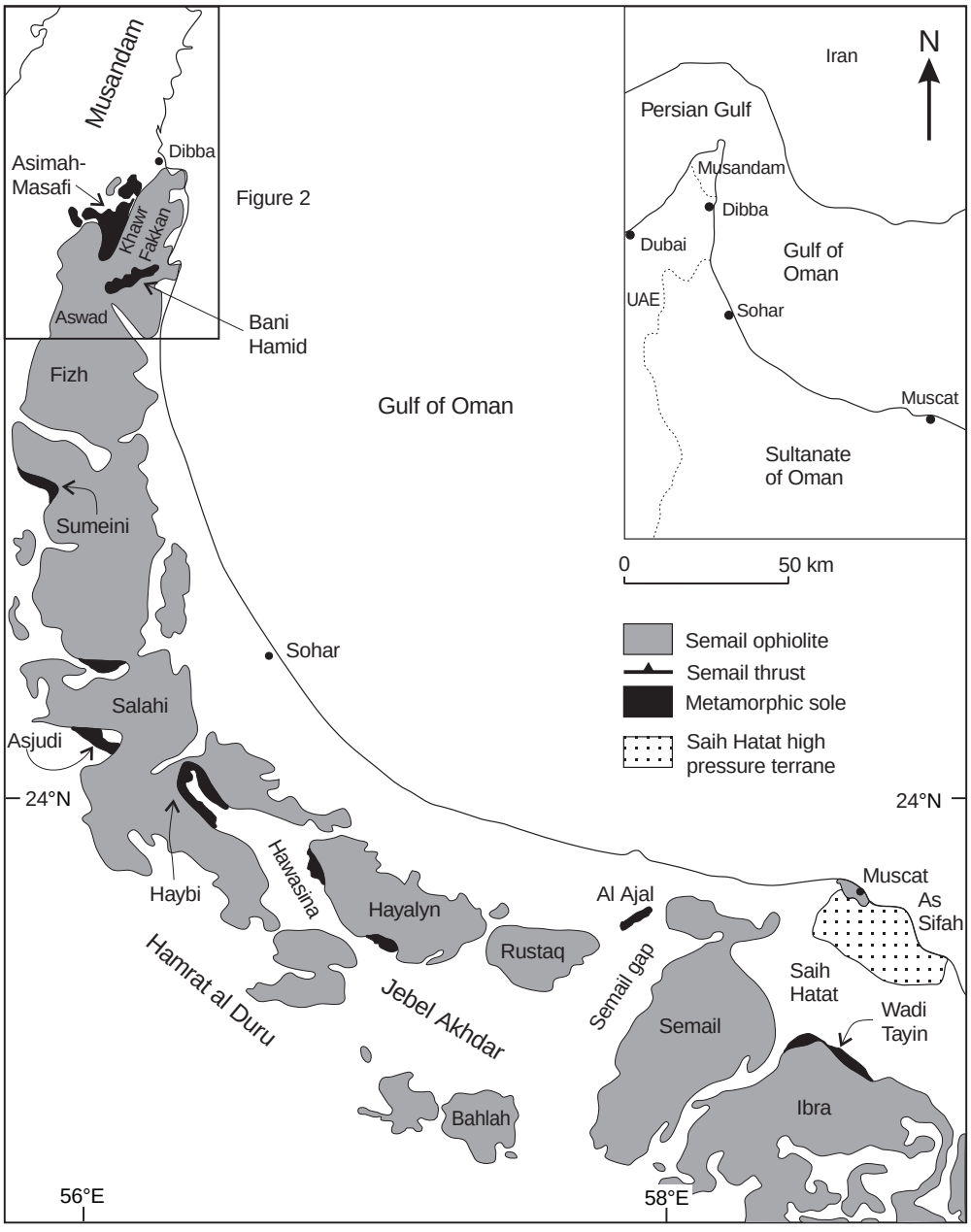

Fig. 1 Map showing the Semail ophiolite of Oman and the United Arab Emirates (UAE), showing the major metamorphic sole localities and the As Sifah eclogites referred to in the text. The major structural blocks of the ophiolite are also shown

1996). Briqueu et al. (1991) concluded that dykes at Ra's Dadnah (Fig. 2) formed from melting during obduction of the metabasalts and metasediments of the ophiolite metamorphic sole. Rare K rich granitoid intrusions in the mantle sequence of the central Oman mountains (Browning 1982; Lippard et al. 1986) were analysed by Pearce (1989) who concluded that they were derived by melting of subducted Arabian margin sediments (Hawasina and Haybi complexes) thrust under the ophiolite.

Leucogranites are characterised by the presence of aluminous minerals like muscovite, biotite, cordierite, garnet, and aluminosilicate polymorphs. They can form extensive bodies resulting from the prograde anatexis of metasedimentary sequences in continental collisional settings like the Himalaya. Such granitoid melts can be produced by a wide variety of mechanisms and from a wide range of source materials. It is generally recognised however that the generation of the majority of peraluminous granitoid bodies has involved the anatexis of sedimentary material (Miller 1985). Generation by the vapour absent partial melting of high grade metapelitic, muscovite rich source materials during continent-continent collision is now widely accepted as the major petrogenetic mechanism for granites of this type (Patiño Douce and Harris 1998).

We report a wide variety of leucogranitic dyke assemblages from the Khawr Fakkan block of the Semail ophiolite in the UAE, including peraluminous garnet-

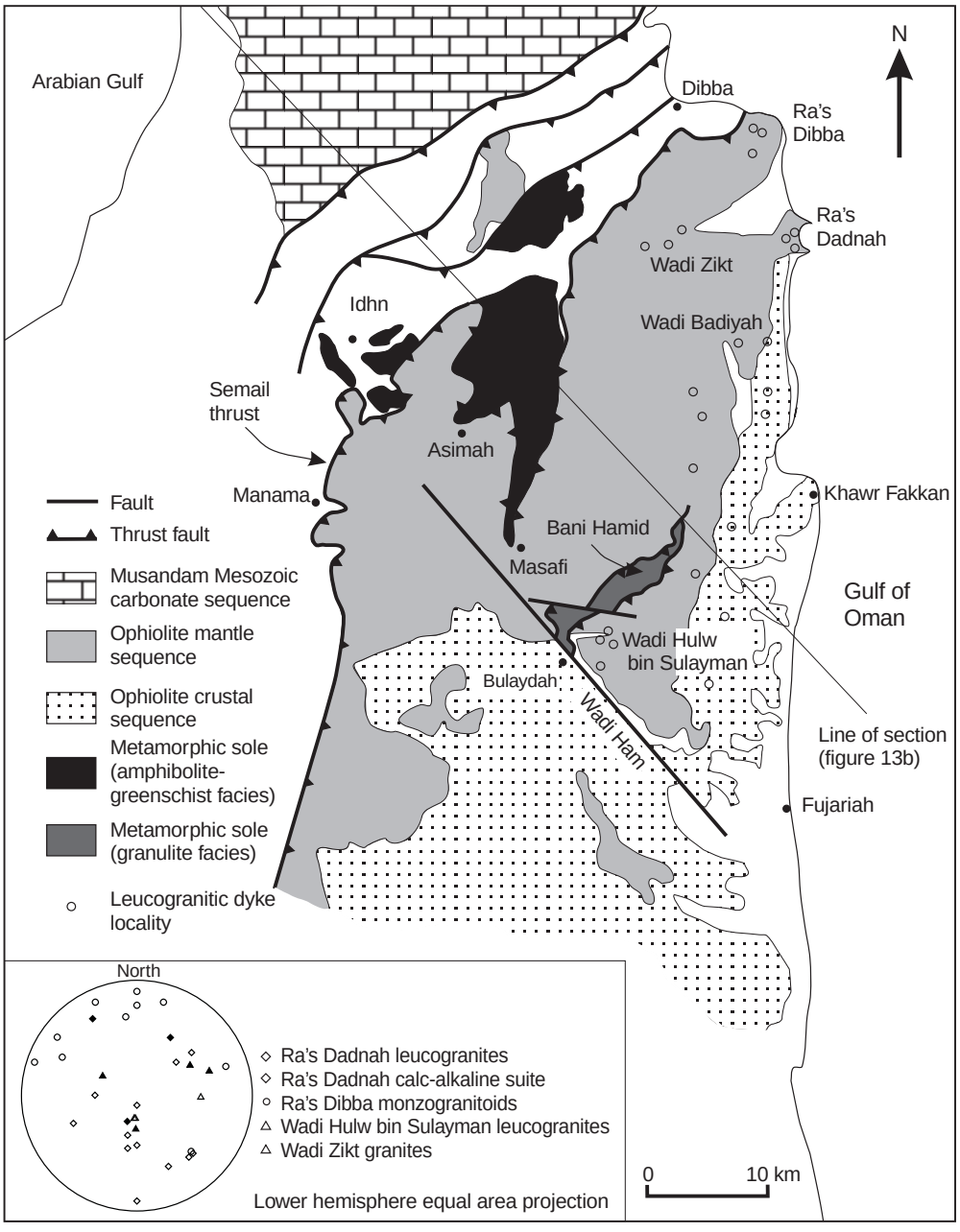

Fig. 2 Generalised geological map of the Khawr Fakkan block of the Semail ophiolite in the UAE, showing the Bani Hamid granulite metamorphic sole unit, the classic sole localities of the Asimah and Masafi region, and the major granitoid dyke localities referred to in the text. See Fig. 1 for location within the Semail ophiolite. *Inset*: stereonet showing the similarity in orientation within individual dyke suites. Some (unsampled) dyke localities after Gnos and Nicolas (1996)

tourmaline and muscovite-biotite leucogranites and andalusite-cordierite monzogranitic pegmatites, in addition to metaluminous to peraluminous quartz diorites, tonalites and biotite granites. New geochemical and isotopic data show that the analysed dykes formed by the melting of trench material at the subduction front beneath the ophiolite. The Sr-Nd isotope systematics are compatible with two component mixing that reflects pre-magmatic mixing between contrasting quartzofeldspathic and basaltic components. The latter source may represent volcanoclastic sediments derived from volcanic islands on the subducting continental margin. A new Sm-Nd isochron age of 98.8 ± 9.5 Ma for a composite granitoid dyke at Ra's Dadnah is indistinguishable from the formation age of the ophiolite crust.

Metamorphism associated with ophiolite emplacement

The metamorphic sole along the base of the Semail ophiolite commonly forms, in the southern and central Oman mountains (Fig. 1), a discrete thrust sheet typically ~200 m thick (Searle 1980). The sole exhibits a steep, inverted thermal gradient from garnet-diopside amphibolites at the peridotite contact, downwards through plagioclase-hornblende and epidote amphibolites, to a variety of greenschist facies metasediments,

mainly quartzites and marbles, with subordinate volcanoclastic and carbonate units. Small volumes of partial melting occur at the highest grade parts of the metamorphic sole where cm to m scale melt pods and veins of hornblende tonalite melts intrude garnet-diopside amphibolites (Searle and Malpas 1980, 1982). The presence of metamorphic sole outcrops beneath both the leading and trailing edges of the ophiolite (Fig. 1) implies that the sole extends beneath the entire ophiolite. The strong deformational fabrics seen within the metamorphic sole, particularly at higher structural levels, are parallel to the Semail thrust and similar to fabrics in the lower ''banded ultramafic unit'' of the ophiolite (Searle 1980). This structural evidence is reinforced by recent geochronological data (Hacker et al. 1996) and is compatible with the contemporaneous formation of the metamorphic sole and initial detachment of the ophiolite. The ubiquitous nature of the deformation of the metamorphic sole means that the true structural thickness of the sole sequences are difficult to determine. This observation has repercussions for the accuracy of any modelling of the thermal and deformational evolution of the obduction process based on thermometric and geochronological studies of the metamorphic sole. Peak temperatures within the metamorphic sole have been estimated at ~775–875 °C (Searle and Malpas 1980; Ghent and Stout 1981; Hacker and Mosenfelder 1996) although the absence of true pelitic assemblages has meant peak pressures are less well constrained. Thermobarometry and structural considerations indicate minimum pressures of ~5 kbar at Wadi Tayin (Ghent and Stout 1981). However, the presence of kyanite and quartz in metabasaltic amphibolites from the Asimah–Masafi sole in the UAE has recently enabled higher peak pressures of 11 ± 2 kbar to be estimated (Gnos 1998).

Many hornblende $^{40}Ar/^{39}Ar$ and K-Ar ages from Semail ophiolite metamorphic sole amphibolites have been determined (Alleman and Peters 1972; Hacker 1994; Lanphere et al. 1981; Lippard et al. 1986; Montigny et al. 1988; Gnos and Peters 1993) with results ranging from 101 to 89 Ma and clustering around 98 Ma. Recent $^{40}Ar/^{39}Ar$ ages of hornblendes from amphibolites in the metamorphic sole have a mean of 94.9 ± 0.2 Ma in the UAE and a slightly younger mean of 93.5 ± 0.1 Ma in Oman (Hacker et al. 1996). The U-Pb zircon ages from plagiogranites (late-stage differentiates of the plutonic sequence) in the Semail ophiolite have a mean of 94.8 ± 0.1 Ma (Tilton et al. 1981) and are interpreted as recording the formation of the ophiolitic crust. The overlap between these ages indicates that obduction, accompanied by the initial, highest grades of metamorphism, was initiated at the same time as or immediately after the crystallisation of the ophiolite – although not necessarily synchronously along the length of the ophiolite.

In the Khawr Fakkan block of the ophiolite in the UAE (Fig. 1), normal garnet-diopside amphibolite facies metabasalts and lower grade metasedimentary and volcanic units (mostly metaquartzites with lesser volumes of metabasic and metacarbonate rocks), occur in the heavily imbricated and folded Dibba zone and Masafi corridor (Fig. 2). An outcrop width of ~6 km of sub-ophiolite metamorphic rocks has been described (Alleman and Peters 1972; Searle 1980). Peak temperatures of 800 ± 100 °C (Gnos 1992) are similar to estimates from the classic Wadi Tayin (Ghent and Stout 1981) and Sumeini (Searle 1980) localities (Fig. 1). Isotopic and geochemical work on the Asimah metavolcanic sequence (Zeigler et al. 1991) have demonstrated the equivalence of these greenschist facies units and unmetamorphosed Triassic and Jurassic volcanics found in the Haybi thrust sheet (Searle 1980) that underlies the Semail ophiolite.

In the Bani Hamid area (Fig. 2), a sequence of wholly granulite facies rocks with an apparent structural thickness of ~1 km is found in a different structural position to the Asimah sole. Field mapping indicates that this heavily imbricated sequence was exhumed along a major out of sequence thrust that repeats the entire ophiolite mantle sequence (Searle and Cox 1999) and did not form in a transform fault pull apart basin as proposed by Gnos and Nicolas (1996). The presence of abundant enstatite-cordierite-sillimanite-spinel ± sapphirine quartzites, alkaline mafic granulites and calc-silicate assemblages are unique to Bani Hamid (Bucher and Kurz 1991; Gnos 1992; Gnos and Kurz 1994; Searle and Cox 1999). The base of the sequence is dominated by basic granulites and quartzofeldspathic gneisses, while calc-silicates are more common towards the top of the sequence, adjacent to the Semail thrust. The rocks all exhibit granulite facies assemblages, and the steep inverted metamorphic gradient seen in the classic metamorphic sole is absent. Estimated peak conditions of equilibration are 800 ± 50 °C and 6.5–9 kbar (Gnos and Kurz 1994), and coronae and symplectites in garnet-diopside-scapolite-plagioclase ± wollastonite calc-silicates are consistent with an anticlockwise *PT* evolution (Searle and Cox 1999). Rare partial melt segregations, petrographically distinct from the leucogranitic dykes, have been described from mafic granulites (enstatite-diopside-hornblende ± plagioclase) in the Bani Hamid sequence (Searle 1980). Alkali and Ti rich mafic granulite sills (with ultramafic xenoliths) within metacarbonatite units of the Bani Hamid terrain may be correlated with similar alkalic metavolcanics described from the Asimah terrain (Zeigler et al. 1991). It is likely that the Asimah (greenschist) and Bani Hamid (granulite) sole terrains represent the metamorphosed equivalents of the unmetamorphosed Permo-Triassic and Jurassic Haybi volcanics observed beneath the Semail ophiolite in the Oman mountains (Searle 1980, 1984).

The age of this granulite facies sequence relative to the adjacent Asimah sole terrain is unclear. A K/Ar hornblende age of 95.3 ± 0.5 Ma (Gnos and Peters 1993) from a Bani Hamid metabasic granulite overlaps the mean hornblende age of 94.9 ± 0.2 Ma for the amphibolite facies metamorphism in the Asimah area (Hacker et al. 1996). The likely equivalence of the Bani

Hamid and Asimah terrains and the Haybi complex implies that Permo-Triassic and Jurassic transitional oceanic crustal material was subducting NE beneath the obducting Semail ophiolite. Furthermore, the presence of the Haybi complex beneath the entire Semail ophiolite may imply the presence of granulite facies metamorphic material at depth throughout the ophiolite belt. The exhumation of the Bani Hamid terrain due to localised, late, out of sequence thrusting may be related to the early Tertiary formation of the adjacent Musandam culmination.

Leucogranitic dykes intruding the ophiolite

Field relations and petrography

A few minor granitic dykes intrude the Semail ophiolite sequence in the Rustaq block in the central Oman mountains and are composed of quartz-plagioclase-alkali feldspar-biotite with minor amounts of green amphibole, prehnite, epidote and magnetite (Browning 1982; Lippard et al. 1986; Pearce 1989). These biotite granites occur as dykes and lenses in NW–SE trending shear zones in the uppermost mantle and lower crustal sequence. They are geochemically distinct from the trondhjemites which form the final end member fractionates of the ophiolite late intrusive series in mid or upper crustal levels. Pegmatoid leucogranitic dykes appear to be restricted to the northernmost part of the Semail ophiolite in the Khawr Fakkan block (Fig. 2). Here granitoid intrusions are widespread and occur as irregular and often anastomosing dykes or lenses up to 30 m thick (Peters and Kamber 1994; Gnos and Nicolas 1996) intruding tectonised serpentinised harzburgites and cumulate gabbros of the upper mantle and lower crustal sequences. They clearly postdate mantle fabrics in the harzburgites and igneous layering in the gabbro cumulates.

Dykes were sampled from a large composite body at Ra's Dadnah, Ra's Dibba and Wadi Hulw bin Sulayman adjacent to the Bani Hamid terrain (Fig. 2). Each locality is dominated by a particular granitoid paragenesis: hornblende-biotite diorites to biotite granites and garnet leucogranites (forming a large composite sill), cordierite-andalusite monzogranites, and garnet-tourmaline with biotite-muscovite leucogranites respectively. No cross cutting relationships between different leucogranite assemblages were observed. Peters and Kamber (1994) have also described garnet-tourmaline leucogranites intruding the Bani Hamid metamorphics at Bulaydah in Wadi Ham.

In the Ra's Dadnah composite sill, the increase in quartz content from diorites through tonalites to granites is accompanied by an increase in the presence of perthitic alkali feldspar, the replacement of amphibole by biotite and a fall in the Ca content of plagioclase from An_{50} to An_{20}. The presence of a late anhedral generation of albite ($An_{5–15}$) overgrowing zoned euhedral plagioclase crystals ($An_{35–25}$) suggests that sub-solidus metasomatic albitisation of potassium feldspars occurred (Briqueu et al. 1991). The marginal leucogranitic components of the Ra's Dadnah composite body contain abundant skeletal, spessartine rich garnet and occasional tourmaline.

At Ra's Dibba (Fig. 2), a suite of more homogeneous and mesocratic pegmatitic dykes contains abundant cordierite and andalusite with inclusions of staurolite and hercynite (Peters and Kamber 1994), rare biotite and secondary muscovite. The felsic assemblage is restricted to quartz graphically intergrown with a perthitic or rarely anti-perthitic feldspar. Grain sizes in these pegmatitic granitoids can reach 30 cm.

In Wadi Hulw bin Sulayman granitoid intrusions are common, with fine grained, homogeneous and often mylonitised biotite granites predominating and exhibiting a genetic relationship with enclosed pegmatitic segregations of garnet-tourmaline bearing, leucogranitic material.

Many dykes exhibit a multistage history with margin parallel zonation (Peters and Kamber 1994). From field relations this can be ascribed both to *in situ* differentiation (e.g. the presence of garnet-tourmaline and muscovite leucogranite veins and segregations within biotite granites) and to the exploitation of the same melt channels by discrete melt pulses. Xenoliths are common in all dyke localities. Most are of wall rock mantle sequence material, as well as cogenetic granitic material in larger composite dykes. Rare metasedimentary material, both restitic garnet-biotite aggregates and unassimilated banded quartzitic enclaves, has been observed in some leucogranitic dykes in Wadi Hulw bin Sulayman. The presence of these enclaves suggests the adjacent Bani Hamid terrain as a potential source for the granitoids.

Deformation and metamorphism of granite dykes to produce gneissic and mylonitic fabrics is widespread, accompanied by low grade metamorphism with the development of albite (replacing potassium feldspar), prehnite, pumpellyite, chlorite and epidote-clinozoisite. This deformation is most intense in regions of serpentinised country rock.

Analytical techniques

Major and trace element analyses were determined by X-ray fluorescence (XRF) spectrometry (Philips PW 1404) at the University of Bergen using glass beads and pressed-powder pellets respectively, with an accuracy of 1% for major elements and ± 10 ppm for trace elements. The typical quoted XRF detection limits (Table 1a) are from Potts (1987). The % FeO was determined from total Fe (as Fe^{3+}) by standard titration methods.

The Sr and Nd isotopes were measured at the University of Bergen on a Finnigan 262 mass-spectrometer. The chemical processing was carried out in a clean-room environment with HEPA filtered air supply and positive pressure, and the reagents were purified in two bottle Teflon stills. Samples were dissolved in a mixture of HF and HNO_3. The Sr and Rb were separated by specific extraction chromatography using the method described by Pin et al. (1994). Strontium was loaded on a double filament and analysed in static mode. Repeated measurements of the NBS 987 Sr standard at the time of this study yielded an average of 0.710252 ± 19 (2σ) ($n = 30$); the accepted value is 0.710240.

The REE were separated by specific extraction chromatography using the method described by Pin et al. (1994). The Sm and Nd were subsequently separated using a modified version of the method described by Richard et al. (1976). The Sm and Nd were loaded on a double filament and analysed in static and dynamic mode respectively. The Nd isotopic ratios were corrected for mass fractionation using a $^{146}Nd/^{144}Nd$ ratio of 0.7219. The Sm and Nd concentrations were determined using a mixed $^{150}Nd/^{149}Sm$ spike. Repeated measurements of the Johnson and Matthey Nd_{203} oxide (batch #S819093A) yielded an average $^{143}Nd/^{144}Nd$ ratio of 0.511120 ± 10 (2σ) ($n = 17$).

Major and trace element geochemistry

With the exception of sample OM 77 all the studied granitoids occupy a narrow range in SiO_2 content of 72–76%. Within individual suites (such as the Ra's Dadnah composite sill) the observed linear inverse correlations between Si contents and Al, Fe and Mg content (Fig. 3a–d) may be indicative of *in situ* fractional crystallisation of feldspars and biotite. Field and petrographic evidence is generally consistent with this interpretation. However, such linear correlations are controversial and other mechanisms invoked to account for them include the progressive incorporation of restitic phases (Chappell and White 1992) or multi-stage partial melting (Holtz and Barbey 1991). All may be true in

Table 1 a Major and trace element geochemistry of the sampled granitoids. F201, OM 620a and OM 628 are from Peters and Kamber (1994)

Sample:	OM 79	JC 11	OM 85	JC 25	OM 77	JC 31	JC 33	JC 112	OM 620a	OM 94	OM 91	OM 628	OM 92	F 201	OM 98	OM 124	OM 125	OM 120	OM 119	OM 118	OM 99	Typical XRF detection limits
	Ra's Dadnah leucogranites				Ra's Dadnah calc alkaline suite				Ra's Dibba monzogranitoids							Wadi Hulw bin Sulayman leucogranites					Wodi Zilot	
Major elements (wt%)																						
SiO_2	75.97	76.10	76.71	76.76	63.63	72.49	74.09	74.47	72.16	72.84	73.54	73.87	74.14	74.21	76.09	74.07	74.59	74.69	74.83	75.21	76.34	0.032
TiO_2	0.03	0.02	0.03	0.02	0.24	0.19	0.15	0.15	0.10	0.20	0.07	0.06	0.12	0.11	0.09	0.08	0.05	0.05	0.07	0.14	0.04	0.001
Al_2O_3	13.64	12.75	12.79	12.93	15.54	14.06	13.07	13.21	12.29	14.58	13.32	12.94	14.01	13.96	13.36	13.19	13.43	13.62	13.18	13.09	13.32	0.078
Fe_2O_3	0.11	0.07	0.03	0.27	1.85	0.47	0.75	0.78	0.37	0.95	0.01	0.02	0.51	0.70	0.27	0.00	0.14	0.31	0.12	0.50	0.02	0.004
FeO	0.36	0.18	0.29	0.29	4.75	0.94	1.44	1.37	0.36	1.22	0.14	0.30	0.76	0.36	0.40	0.32	0.27	0.58	0.34	0.58	0.29	0.004
MnO	0.03	0.00	0.16	0.32	0.13	0.03	0.07	0.05	0.04	0.17	0.00	0.02	0.10	0.09	0.04	0.09	0.41	0.66	0.09	0.10	0.02	0.001
Mgo	0.00	0.31	0.00	0.16	2.85	1.01	0.75	0.75	0.03	0.47	0.59	0.40	0.18	0.13	0.09	0.45	0.06	0.05	0.25	0.62	0.20	0.075
CaO	2.01	5.61	1.36	2.47	6.00	5.55	2.54	2.23	0.29	0.32	0.62	2.02	0.24	0.23	0.33	0.93	1.11	0.65	0.97	1.03	1.83	0.012
Na_2O	6.81	3.39	7.82	5.27	2.47	3.14	5.74	4.63	8.61	4.69	8.28	7.56	5.32	4.81	5.24	4.76	4.13	6.02	4.04	3.14	5.40	0.233
K_2O	0.23	0.14	0.23	0.14	0.28	0.09	0.26	1.02	4.11	2.54	2.92	0.82	3.41	3.67	3.31	5.23	4.61	1.87	5.10	4.82	1.64	0.021
P_2O_5	0.02	0.00	0.00	0.00	0.06	0.11	0.08	0.05	0.05	0.06	0.07	0.03	0.04	0.04	0.03	0.03	0.05	0.05	0.05	0.04	0.02	0.031
H_2O etc	0.43	1.33	0.35	1.01	2.19	1.76	0.96	0.95	0.73	1.12	0.58	1.08	0.85	0.92	0.47	0.54	0.83	0.92	0.51	0.36	0.57	–
Total	99.64	99.90	99.77	99.59	99.99	99.84	99.90	99.66	99.14	99.16	100.14	99.12	99.68	99.23	99.72	99.69	99.68	99.47	99.55	99.63	99.69	–
Trace elements (ppm)																						
S	2300	8700	2300	2400	3100	8500	3100	3400	2200	2200	2300	2400	4200	2200	2200	2300	2600	2400	2400	2500	2500	20
V	5	2	2	2	178	54	43	39	7	2	2	4	2	2	2	12	10	2	10	32	3	2
Cr	2	2	2	2	37	10	14	2	2	2	2	2	2	2	2	2	2	2	2	2	2	2
Co	2	5	2	6	34	12	13	16	2	5	2	2	2	4	2	2	2	2	2	3	2	6
Ni	2	4	4	5	29	23	14	8	2	2	2	2	5	2	2	6	5	2	4	8	2	6
Cu	49	33	37	49	146	48	44	46	39	42	40	41	40	33	40	29	31	38	37	76	35	6
Zn	11	8	10	13	73	19	33	25	11	31	11	11	27	23	14	16	17	26	15	32	12	9
Rb	2	4	1	2	6	1	4	17	46	43	101	13	65	101	38	129	156	111	129	139	27	3
Sr	59	103	35	68	145	206	152	128	12	11	28	190	20	400	3	39	50	13	56	76	168	3
Y	107	13	166	155	25	15	27	23	33	47	8	22	79	69	33	20	28	36	24	46	24	3
Zr	110	76	72	77	64	122	100	99	51	106	22	91	66	64	48	46	62	45	55	89	62	6
Nb	20	12	64	33	9	8	13	14	39	91	12	6	43	45	36	8	8	44	12	15	7	6
Ba	2	2	2	2	44	51	20	74	2	74	70	389	15	29	2	20	51	14	7	85	406	7
La	7	4	11	5	6	2	9	11	14	15	7	7	3	11	7	10	12	8	11	18	7	3
Ce	6	2	34	21	6	120	7	40	2	2	4	13	5	2	6	2	2	2	5	19	7	8
Nd	10	2	16	21	9	40	8	15	6	10	7	10	11	7	7	20	5	14	8	20	8	6

Table 1 b Modal mineralogy and CIPW norms of the sampled granitoids

Sample:	OM 79	JC 11	OM 85	JC 25	OM 77	JC 31	JC 33	JC 112	OM 620a	OM 94	OM 91	OM 628	OM 92	F 201	OM 98	OM 124	OM 125	OM 120	OM 119	OM 118	OM 99
	Ra's Dadnah leucogranites				Ra's Dadnah calc alkaline suite				Ra's Dibba monzogranitoids							Wadi Hulw bin Sulayman leucogranites					Wadi Zikt
CIPW norms (wt%)																					
Quartz	31.88	45.13	29.62	39.90	28.05	40.95	36.73	37.11	24.71	35.22	24.38	25.87	29.70	31.52	31.95	25.23	30.31	30.71	29.76	35.19	34..66
Orthoclase	1.36	0.83	1.64	0.83	1.66	0.53	6.06	6.06	23.30	15.00	17.24	4.84	20.13	21.68	19.57	30.91	27.24	10.56	30.02	28.36	9.70
Albite	57.54	28.61	64.43	44.54	20.88	26.51	39.14	39.14	39.24	39.61	51.19	61.94	44.96	40.66	44.28	38.62	34.90	50.83	34.06	26.72	45.64
Anorthite	5.96	19.16	0.00	11.21	29.42	23.98	10.74	10.74	0.00	1.58	0.00	0.00	1.20	1.14	1.64	0.00	4.46	2.90	2.83	4.86	7.24
Corundum	0.00	0.00	0.00	0.00	0.38	0.00	0.54	0.54	0.00	3.53	0.00	0.00	1.12	1.66	0.55	0.00	0.00	0.72	0.00	0.90	0.00
Acmite	0.00	0.00	0.09	0.00	0.00	0.00	0.00	0.00	1.06	0.00	0.03	0.06	0.00	0.00	0.00	0.00	0.00	0.00	0.00	0.00	0.00
Sodium metasilicate	0.00	0.00	0.54	0.00	0.00	0.00	0.00	0.00	9.98	0.00	3.54	0.68	0.00	0.00	0.00	0.57	0.00	0.00	0.00	0.00	0.00
Diopside	1.08	2.29	1.46	0.89	0.00	2.28	0.00	0.00	1.27	0.00	2.31	3.19	0.00	0.00	0.00	3.65	0.63	0.00	1.22	0.00	1.41
Wottustonite	1.12	2.44	2.13	0.00	0.00	0.00	0.00	0.00	0.00	0.00	0.00	2.50	0.00	0.00	0.00	0.00	0.00	0.00	0.00	0.00	0.00
Hypasstruene	0.00	0.00	0.00	0.81	14.15	2.51	3.58	3.59	0.14	2.51	0.51	0.00	1.40	0.38	0.65	0.57	0.88	2.08	0.63	2.16	0.29
Magnetite	0.16	0.11	0.00	0.39	2.69	0.68	1.13	1.13	0.00	1.39	0.00	0.00	0.74	1.02	0.39	0.00	0.20	0.44	0.17	0.73	0.03
Ilreaite	0.06	0.04	0.06	0.04	0.46	0.36	0.29	0.29	0.19	0.38	0.27	0.11	0.23	0.21	0.17	0.15	0.010	0.10	0.13	0.27	0.08
Apatite	0.04	0.00	0.00	0.00	0.12	0.24	0.11	0.11	0.11	0.12	0.67	0.06	0.09	0.09	0.06	0.07	0.11	0.11	0.11	0.09	0.04
Total	99.20	98.61	99.97	98.61	97.81	98.04	98.32	98.71	100.00	99.34	100.14	99.25	99.57	98.36	99.26	99.77	98.83	98.45	98.93	99.28	99.09
Mineralogy (vol%)																					
Quartz	30	60	45	55	5	40	40	35	25	50	45	50	50	20	60	30	40	25	35	30	35
Keldopar	5	5	5	5	–	5	10	10	60	35	40	10	30	40	30	40	30	25	35	40	30
Plagioclase	50	30	40	30	50	35	35	50	–	–	–	30	–	–	–	15	15	35	15	15	25
Biotite	–	–	–	–	5	–	10	–	5	–	–	5	–	20	–	5	5	–	5	10	7
Mescorite	–	–	–	–	–	–	–	–	–	–	–	–		–	–	5	5	–	5	5	3
Cordarited	–	–	–	–	–	–	–	–	–	10	5	5	5	15	5	–	–	–	–	–	–
Anndatasite	–	–	–	–	–	–	–	–	10	–	10	–	15	5	5	–	–	–	–	–	–
Garmatrt	–	–	5	5	–	–	–	–	–	–	–	–	–	–	–	5	–	10	3	–	–
Tourralineur	–	–	2	–	–	–	–	–	–	–	–	–	–	–	–	–	–	5	2	–	–
Other[a]	Chl: 15	Chl: 5	Chl: 5	Chl: 3	Chl: 10; Hbl: 30	Chl: 20	Chl: 5	Chl: 10	–	Ore: 5	–	–	–	–	–	–	Chl: 5	–	–	–	–

[a] (*Chl* chlorite, *Hbl* hornblende)

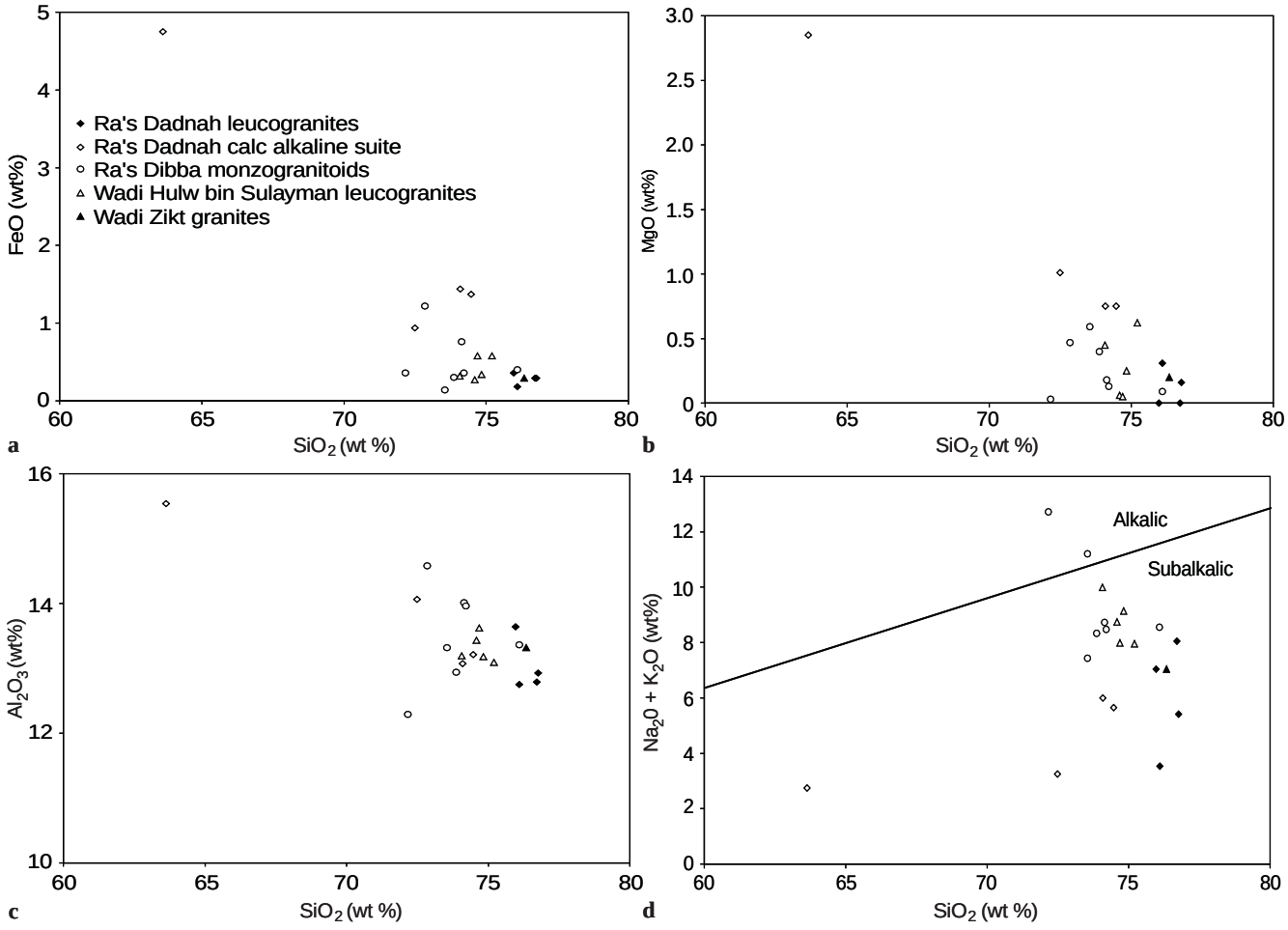

Fig. 3a–d Harker SiO_2 variation diagrams for FeO, MgO, Al_2O_3 and total alkalis. Note the low alkali contents of the components of the Ra's Dadnah composite sill which has undergone greenschist facies metamorphism

specific instances, and field evidence (the presence of garnet-biotite restitic enclaves within dykes) compatible with the restite unmixing model has been observed. The components of the Ra's Dadnah sill also exhibit very low (typically $<0.25\%$) K_2O contents due to metasomatic replacement of potassium feldspar by albite (Briqueu et al. 1991). The Nd-Sr isotopic signature of these dyke components distinguishes them from typical oceanic plagiogranites, as does their position within the ophiolite stratigraphy. Samples from Ra's Dibba are similarly affected, which may account for the high $^{87}Sr/^{86}Sr$ ratios and normative sodium metasilicate of these dykes.

The nature of the relationship between melt geochemistry and magmatic differentiation varies among the dyke suites, although these relationships have been distorted somewhat by subsequent metasomatism (Fig. 4a). The andalusite-cordierite monzogranitoids of Ra's Dibba exhibit a small increase in peraluminous character with differentiation (Fig. 4b). Similar trends are observed in cordierite bearing granitoids from the Hercynides and Himalaya (e.g. LeFort et al. 1987). The intermediate and granodioritic components of the Ra's Dadnah composite sill show a slight decrease in peraluminous character with differentiation. In contrast, the leucogranitic components of the sill exhibit a large variation in [A/CNK], although values increase strongly with differentiation, as do those of the Wadi Hulw bin Sulayman biotite granites and garnet-tourmaline and muscovite-biotite leucogranites. Similar trends have been observed in two mica leucogranitic bodies such as the Manaslu granite of the Nepal Himalaya (LeFort et al. 1987).

The trace element data (Fig. 5) for the granitoid dykes have been normalised to a standard ocean ridge granite (ORG) that represents a pure crystal fractionate of mantle origin (Pearce et al. 1984). Each distinct dyke paragenesis is represented separately for ease of comparison. Each dyke dataset occupies a relatively narrow range for most plotted elements although there are differences among individual dyke parageneses. The Wadi Hulw bin Sulayman leucogranites at the base of the Khawr Fakkan block exhibit the strong LILE enrichment, negative Ba anomaly (probably due to the fractional crystallisation of biotite and potassium feldspar) and low HFSE (Zr, Sm, Y) abundances characteristic of syn-collisional granitoids. Their trace element patterns

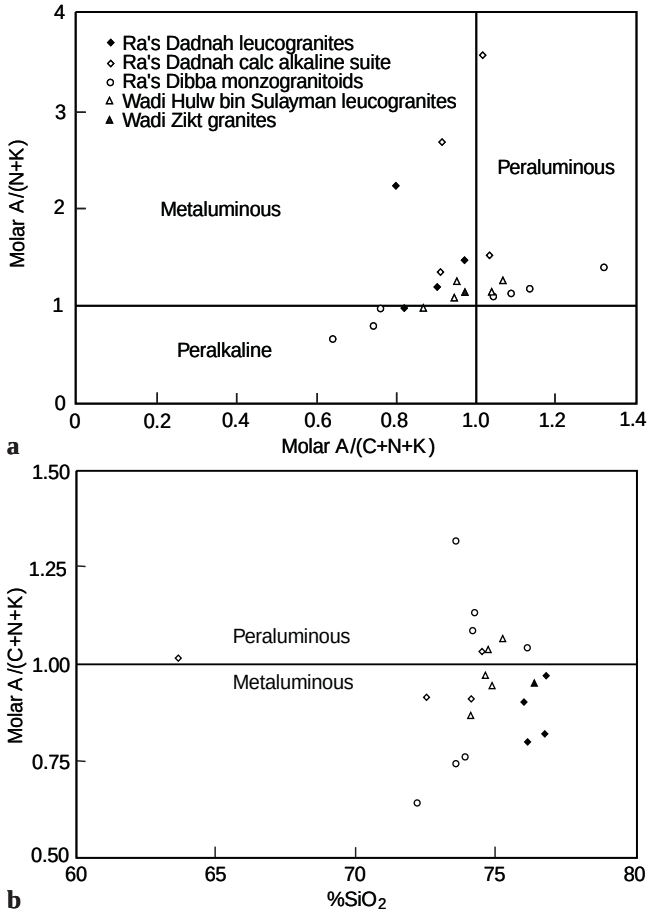

Fig. 4 **a** Diagram showing distribution of granitoids in [A/NK] and [A/CNK] space. The low ($<0.5\%$) K_2O contents of some of the Ra's Dadnah samples can be attributed to post emplacement, fluid driven albitisation of potassium feldspar. **b** Diagram showing the variation of peraluminous character with differentiation, represented by wt% SiO_2. Each mineralogical assemblage exhibits a different trend. See text for discussion

are consistent with derivation from the partial melting of a sedimentary protolith and are similar to those of Himalayan type syn-collisional granites derived from metasedimentary material (Fig. 5). The Ra's Dibba monzogranitoids also have trace element distributions that closely match typical syn-collisional type leucogranitoids. In contrast, the Semail ophiolite trondhjemite and metamorphic sole leucotonalitic amphibolite partial melt show flat patterns close to that of the hypothetical normalising granite. This is to be expected as both these rocks were ultimately derived from a wholly mantle source.

The Ra's Dadnah composite body is found at a higher structural level than the other described granitoids, in the mantle transition zone, and all samples exhibit flat trace element patterns. Metasomatic leaching of LILE from these outcrops has been described by Briqueu et al. (1991) and may account for the low recorded LILE concentrations, while the slightly increased HFSE concentrations compared with the other analysed granitoids may reflect mixing between "sedimentary" and "mantle" type sources. The leucogranitic components of the Ra's Dadnah composite body have a pronounced negative Ba anomaly, likely to be caused by the fractional crystallisation of biotite and potassium feldspar. The positive Nb anomaly again may reflect the presence of a mantle source in the petrogenesis of this body.

The alteration independent Nb-Y diagram (Fig. 6) of Pearce et al. (1984) is effective at discriminating between tectonic environments in granitoid material. The majority of the analysed granites lie in the volcanic arc/syn-collisional granite field, although those intruded at higher structural levels within the ophiolite mantle sequence (Ra's Dibba and Ra's Dadnah) cluster in the within-plate granite field. Peraluminous granites can, however, inherit widely varying compositions depending on petrogenetic conditions and source component compositions. The fact that some of the analyses extend into the within-plate granite field is consistent with a mantle source component in the petrogenesis of these melts. The analysed dykes are clearly distinct from the Semail ophiolite trondhjemite dataset.

Characterisation of melting processes

The trends defined by major and trace element concentrations of leucogranitic melts, particularly when compared with potential source compositions, can be used to characterise the extent and nature of partial melting processes in leucogranite source regions (Inger and Harris 1993). More recently, they have been used in conjunction with experimental petrology (Patiño Douce and Harris 1998) to show the close relationships between Himalayan leucogranites and their sources, commonly high grade metapelites. Partial melting in such regimes is dominated by the dehydration melting of metasediments without the addition of a fluid phase. The influence of such a phase on the degree of partial melting, restite mineralogy, and the trace element geochemistry (particularly the LILE Sr, Rb and Ba) of melts can be used to characterise the melting and tectonic regimes that govern the petrogenesis of such leucogranites. The LILE (Sr, Rb and Ba) covariations are an important tool in the analysis of granitic melt evolution, since they are partitioned into major granitoid phases like plagioclase, alkali feldspar and biotite. The Wadi Hulw bin Sulayman granitoids have higher ($\sim$10–100) Rb/Sr ratios than the Ra's Dadnah suites, which have typical values of $\sim$0.01–0.1 (Fig. 7). Inger and Harris (1993) have argued that such differences may be attributed to different melt processes, with high Rb/Sr ratios resulting from dehydration melting, and lower values, coupled with higher Ba concentrations, resulting from H_2O fluxed melting, which produces a higher proportion of restitic alkali feldspar. Since the ophiolite in the Ra's Dadnah area is heavily deformed and sheared, these lines of weakness in the country rock may have facilitated the input of excess

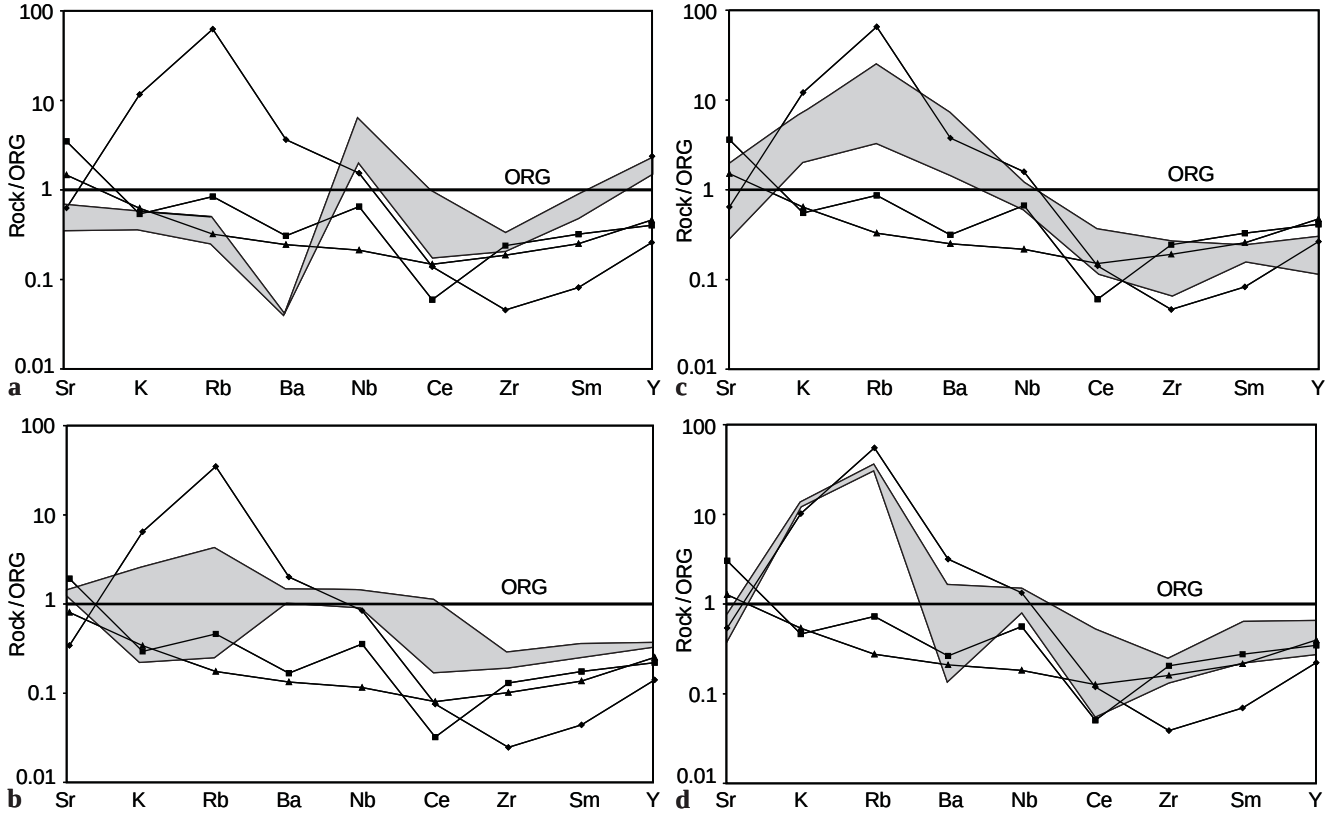

Fig. 5a–d ORG normalised trace element patterns of the analysed granitoids from the Khawr Fakkan block. **a** Ra's Dadnah composite sill leucogranites; **b** Ra's Dadnah composite sill calc alkaline components; **c** Ra's Dibba monzogranitoids; **d** Wadi Hulw bin Sulayman leucogranites. All are compared with –◆– a typical Himalayan metasedimentary melt leucogranite (Searle and Fryer 1986), –■– a partial melt from the amphibolite unit of the Semail ophiolite metamorphic sole (Searle and Malpas 1982), and –▲– a late-stage trondhjemitic fractionate from the upper crustal units of the Semail ophiolite (Lippard et al. 1986). After Pearce et al. (1984)

fluid into melts emplaced locally. We infer that the Wadi Hulw bin Sulayman granitoids were generated by dehydration melting, with minimal added fluid, whereas the Ra's Dadnah suites may have been influenced by excess fluid added to melts emplaced into a sheared part of the ophiolite thrust sheet. However post emplacement LILE leaching makes these conclusions equivocal. Linear trends of Rb/Sr against Sr and Ba (Fig. 7) suggest that *intra-suite* variation is largely a result of fractional crystallisation of biotite and alkali feldspar from a melt source corresponding to the average composition of the underlying Bani Hamid quartzose granulites. The Wadi Hulw bin Sulayman and Ra's Dibba suite trends match the calculated vapour absent partial melting of muscovite trend, resulting in the crystallisation of alkali feldspar. Post emplacement metasomatism of the Ra's Dadnah body makes any such interpretation uncertain.

The relative CIPW normative proportions of Ab, Or and An, plotted on a ternary diagram (Fig. 8a), can be used to differentiate among various granitoid types (Barker 1979). It should be noted that the alkali metasomatism apparent in the components of the Ra's Dadnah composite sill renders any petrogenetic interpretations equivocal. The largely unaltered dykes of the Wadi Hulw bin Sulayman and Ra's Dibba domains plot in the granite field. In recent experimental work (Patiño Douce and Harris 1998), similar granitic compositions (their Fig. 5, p 704) were produced by the dehydration melting of typical Himalayan muscovite and biotite schists, with a fundamental role played by muscovite breakdown. The experimentally derived glass compositions produced were independent of pressure. The addition of a small (1–4 wt%) amount of H_2O to the melting experiments produced tonalitic compositions due to enhanced melting of source plagioclase in the presence of excess H_2O. This evidence is compatible with the conclusion that the Wadi Hulw bin Sulayman leucogranites are near minimum melt leucogranites produced by the dehydration melting of muscovite-biotite bearing quartzofeldspathic schists. In contrast, the Ra's Dibba andalusite-cordierite minimum melt monzogranitoids may have formed in the presence of ~2% excess H_2O.

The CIPW normative compositions of the analysed granitoids (Table 1b) plotted in the ternary, water saturated haplogranite system can be compared with experimentally determined data to constrain the physical conditions of granitoid petrogenesis (Fig. 8b). In this system, minimum melt compositions tend to cluster at a point. Figure 8b suggests that the Wadi Hulw bin Sulayman and Ra's Dibba granitoids represent minimum melt type compositions which crystallised at

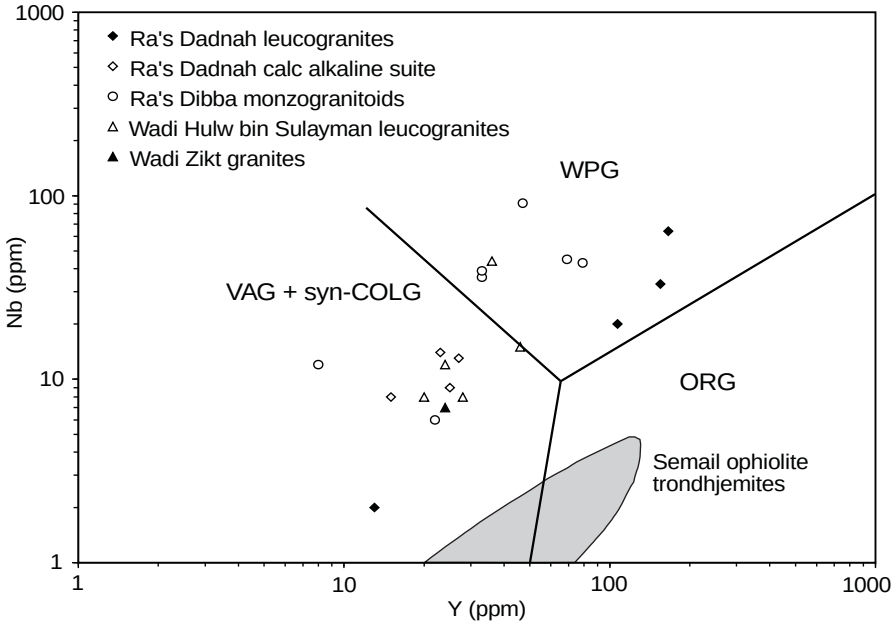

Fig. 6 Tectonic discrimination diagram plotting Nb and Y concentrations, after Pearce et al. (1984) (*Syn-COLG* syn-collisional granites, *VAG* volcanic arc granites, *WPG* within plate granites, *ORG* ocean ridge granites). Semail ophiolite trondhjemite data field from Alabaster et al. (1982). The fact that granitoids from higher structural levels plot in the WPG field is indicative of a mantle component in their petrogenesis

pressures of ~3–4 kbar. This agrees well with the pressure value (2.5 ± 0.1 kbar) for the Ra's Dibba suite determined by Peters and Kamber (1994). The higher inferred values of a_{H_2O} in the Ra's Dibba granitoids are reflected in their pegmatitic nature.

Sr and Nd isotope geochemistry

The Sr and Nd isotope data presented in Table 2 complement the granitoid dykes analysed by Briqueu et al. (1991). A new Sm-Nd isochron age for the large Ra's Dadnah composite dyke is here reported (Fig. 9). Cogenetic components of this large composite sill range from hornblende diorite to garnet leucogranite and generate an isochron [MSWD (mean square of weighted deviates) = 1.18] with an age of 98.8 ± 9.5 Ma and an initial ε_{Nd} value of −4.31. The negative ε_{Nd} values and intermediate to high initial $^{87}Sr/^{86}Sr$ ratios of the analysed granitoids contrast strongly with the published data on the Semail ophiolite (McCulloch et al. 1981). The Ra's Dibba andalusite-cordierite bearing monzogranitoid pegmatites exhibit the highest ε_{Nd} values (typically −1.0) and the most mantle like initial $^{87}Sr/^{86}Sr$ ratios (~0.706). In contrast, the Wadi Hulw bin Sulayman garnet-tourmaline leucogranites exhibit the low ε_{Nd} values (−6.0) and high initial $^{87}Sr/^{86}Sr$ ratios (ε_{Sr} values of 70–80) characteristic of pure metasedimentary melt leucogranites. However, these values are not comparable with Himalayan leucogranites, which have typical ε_{Nd} values of −15 to −20 and ε_{Sr} values of 600–800 (e.g. Inger and Harris 1993). This may reflect a more quartzofeldspathic component in the source region of the Semail leucogranites compared with the metapelitic sources of the Himalayan leucogranites. The complete dataset plots in the "enriched" (+ve ε_{Sr}, −ve ε_{Nd}) quadrant on a ε_{Sr} versus ε_{Nd} diagram (Fig. 10), indicating derivation from a relatively old, LREE enriched (low Sm/Nd), high Rb/Sr source typical of continental crust. The granitoid intrusions define a hyperbolic array, consistent with an origin by the mixing of two distinct source components – a LILE enriched mantle component and a "continental" sedimentary component.

The nature of the continental component

Possible continental end member components involved in the generation of the granitoid dyke suite are Tethyan crustal material subducted beneath the ophiolite (represented by the Haybi complex and metamorphic sole) and the Arabian basement of the passive margin. Numerous arguments suggest that melting of the Arabian basement was unlikely. Estimates indicate that the ophiolite formed as much as 400–500 km offshore (Lippard et al. 1986; Bechennec et al. 1988), and that the ophiolite was not obducted onto the continental margin until ~78 Ma (Hacker et al. 1996). By this time the ophiolite would not have contained enough residual heat to cause anatexis in the underthrust margin. The Sm-Nd isochron age of the Ra's Dadnah body is ~20 Ma older than the continental margin obduction age and therefore precludes melting of the Arabian margin at ~99 Ma. Briqueu et al. (1991) noted that the influence of the Sr rich carbonates of the passive margin would also greatly alter the isotopic characteristics of the granitoids. In the southern Oman mountains, regional H*P* metamorphism in the crust has been ascribed to the subduction of the leading edge of the Arabian continental margin to depths of ~90 km beneath the ophiolite (Searle et al. 1994).

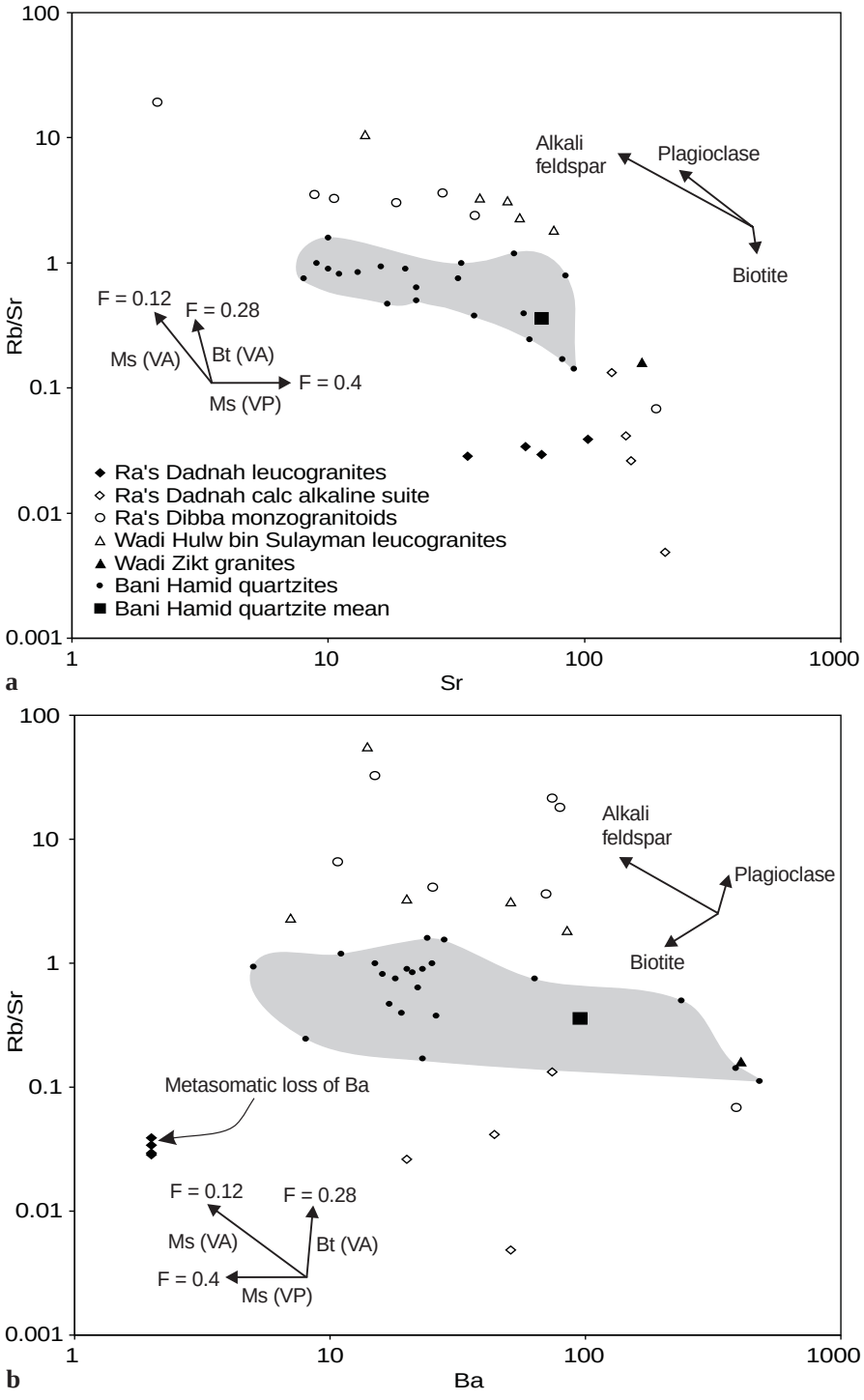

Fig. 7a, b LILE covariation diagrams for Semail ophiolite leucogranitic dykes and Bani Hamid quartzofeldspathic granulite gneisses. Post emplacement alkali metasomatism of the Ra's Dadnah composite body precludes any clear identification of crystallising phases. Vectors represent 10% crystallisation of phase and partial melting reactions (assuming a source containing 20% muscovite and 10% phlogopite). [*F* melt fraction, *Ms* (*VA*) vapour absent muscovite melting, *Ms* (*VP*) vapour present muscovite melting, *Bt*(*VA*) vapour absent biotite melting]. After Inger and Harris (1993) and references therein. Trends defined by the Wadi Hulw bin Sulayman and Ra's Dibba granitoids correspond to the vapour absent melting of muscovite, from a source region similar to the Bani Hamid quartzofeldspathic granulites (data from Briqueu et al. 1991 and Bucher and Kurz 1991)

The Rb-Sr and Sm-Nd isotopic data for granulite facies quartzofeldspathic gneisses from the Bani Hamid metamorphic terrain is presented in Table 2. The juxtaposition of the highest grades of sub-ophiolitic metamorphism seen in the Oman mountains and the high granitoid intrusion density in Wadi Hulw bin Sulayman (Fig. 2) suggests a genetic relationship between the two lithologies. The Wadi Hulw bin Sulayman leucogranites have trace element patterns that are very similar to typical Himalayan leucogranites. The similarity in Nd and Sr isotopic characteristics between the Wadi Hulw bin Sulayman leucogranites and the majority of the analysed Bani Hamid metasediments also suggest they may be closely related. The LILE covariation modelling is compatible with the leucogranites being the products of the vapour absent melting of the Bani Hamid granulites (Fig. 7), and the minimum melt type nature of the leucogranites (Fig. 8) has been demonstrated. Briqueu

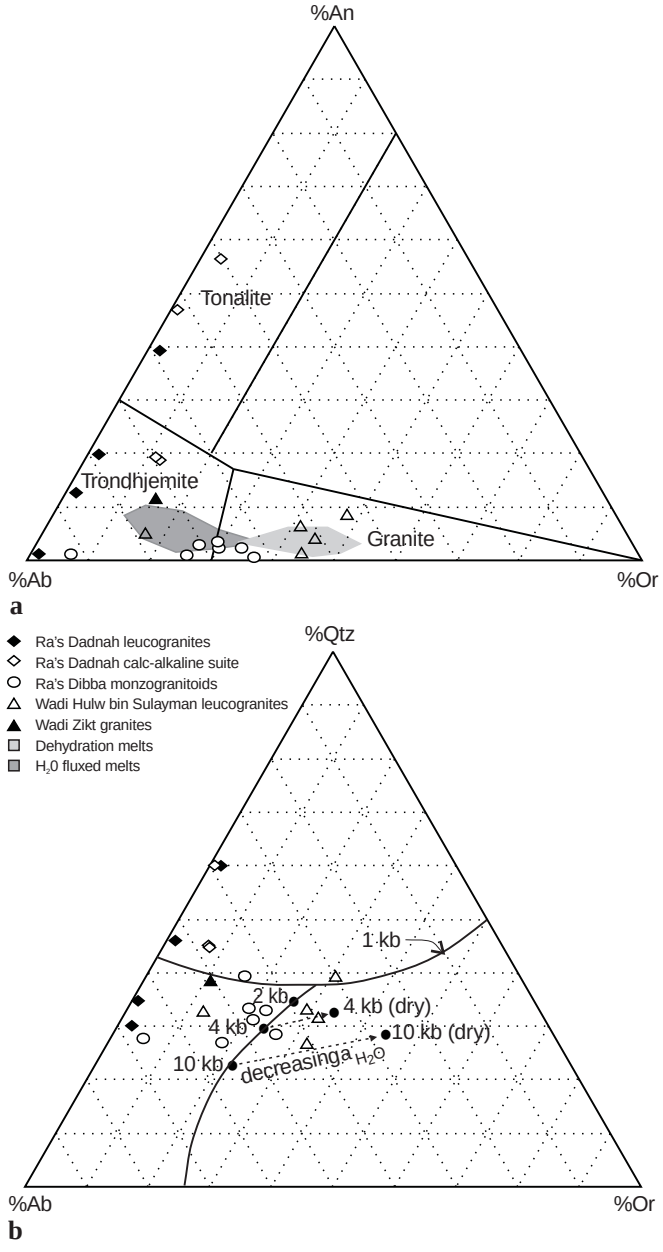

Fig. 8 **a** CIPW normative classification of the analysed leucogranitic dykes, after Barker (1979). Leucogranites from Wadi Hulw bin Sulayman and Ra's Dibba correlate well with the fields defined by experimentally derived glasses formed from typical Himalayan muscovite-biotite schists (Patiño Douce and Harris 1998). Components of the Ra's Dadnah composite body have undergone metasomatic replacement of potassium feldspar by albite. **b** Phase relationships and minimum melt compositions in the CIPW normative system quartz-albite-orthoclase ± H_2O ± anorthite ± F. The clustering of the Wadi Hulw bin Sulayman and Ra's Dibba granitoids suggests a minimum melt composition for both domains, with the former suite crystallising at lower H_2O activity. The metasomatic loss of K_2O from the Ra's Dadnah composite dyke components makes any interpretation of their phase relationships equivocal. Experimental minimum melt compositions from Rollinson (1993) and references therein. Data symbols as Fig. 8a

et al. (1991) demonstrated that the granitoids of the Ra's Dadnah composite sill have Pb isotopic compositions inherited from the Bani Hamid granulites. We propose that the Wadi Hulw bin Sulayman leucogranites and their inferred metasedimentary protoliths in the Bani Hamid terrain represent the continental end member in mixing calculations. The end member used in the mixing model calculations is sample OM 124 (Table 2).

Isotopic disequilibrium in the Rb-Sr system

Isotopic disequilibrium between melt and restite phases during melt generation will occur when the volume diffusion rates of Rb and Sr between phases which accommodate Rb and Sr (micas and plagioclase) are slower than the rate of melt extraction from the source region. Such studies are increasingly used to constrain rates of melt generation in collisional terrains. Harris and Ayres (1998) showed that advective heating and rapid melt extraction from source regions are major causes of isotopic disequilibrium between protoliths and melts, and that disequilibrium is facilitated by rapid protolith heating, although the dynamic recrystallisation that accompanies shearing promotes isotopic re-equilibration. Melt processes also influence the relative $^{87}Sr/^{86}Sr$ ratios of restite and melt. During the vapour absent melting of muscovite, the release of radiogenic Sr from muscovite (which has a high Rb/Sr ratio compared to plagioclase) will cause melts to inherit higher $^{87}Sr/^{86}Sr$ ratios than their source. In contrast, vapour present derived melts contain a greater $^{87}Sr/^{86}Sr$ contribution from plagioclase, which results in minimal disequilibrium between source and melt. Tectonic models suggest that the Semail ophiolite granitoid dyke suite formed under conditions of advective heating (from the residual heat of the ophiolite) and strong shearing. However, the similarity in initial $^{87}Sr/^{86}Sr$ ratios of the proposed metasedimentary source (~0.709–0.710) and the adjacent Wadi Hulw bin Sulayman leucogranites (up to ~0.710), suggest that significant disequilibrium in the subduction zone Rb-Sr system of the leucogranitic dykes can be discounted. We conclude that this may be the result of dynamic recrystallisation of the source sediments during shearing in the subduction zone, coupled with melt extraction slower than the ~0.2 Ma threshold for the preservation of Sr isotopic disequilibrium (Harris and Ayres 1998).

The nature of the mantle component

Possible depleted mantle end member components involved in the generation of the granitoid dyke suite are oceanic or volcanoclastic sediments subducted beneath the ophiolite and the LILE and volatile enriched harzburgitic mantle wedge above the subduction zone. Acceptance of the SSZ origin of the ophiolite precludes the possibility of material identical to the preserved ophiolitic crustal sequence lavas being subducted beneath the ophiolite (Searle and Cox 1999). Subducted crustal material is represented by the unmetamorphosed

Table 2 Sm-Nd and Rb-Sr isotope data of the sampled granitoids. The ε notation follows DePaolo and Wasserburg (1976a), using UR values for Sr from DePaolo and Wasserburg (1976b), and CHUR values for Nd from Jacobsen and Wasserburg (1984). Decay constants from Steiger and Jager (1977)

Sample	Rock unit	Sm (ppm)	Nd (ppm)	$^{147}Sm/^{144}Nd$	$^{143}Nd/^{144}Nd$	$\varepsilon_{Nd(90\ Ma)}$	Rb (ppm)	Sr (ppm)	$^{87}Rb/^{86}Sr$	$^{87}Sr/^{86}Sr$	$^{87}Sr/^{86}Sr_i$ (90 Ma)	$\varepsilon_{Sr(90\ Ma)}$
Khawr Fakkan block granitoids												
OM 79	Ra's Dadnah leucogranites	4.41	10.48	0.255	0.512456 ± 7	−4.2	1.45	58.73	0.071	0.707153 ± 9	0.707062	37.9
OM 85		6.61	15.71	0.254	0.512458 ± 7	−4.2	1.32	34.82	0.10	0.706987 ± 10	0.706847	34.8
JC 25		7.85	20.52	0.231	0.512435 ± 6	−4.4	1.86	68.10	0.079	0.706850 ± 9	0.706749	33.4
OM 77	Ra's Dadnah calc alkaline suite	2.34	8.81	0.161	0.512396 ± 6	−4.3	6.43	144.71	0.129	0.707447 ± 10	0.707282	41.0
JC 31		6.51	40.29	0.098	0.512325 ± 6	−5.0	1.32	206.27	0.019	0.707130 ± 9	0.707106	38.5
JC 112		3.23	14.78	0.132	0.512375 ± 8	−4.4	17.04	127.59	0.386	0.707406 ± 9	0.706912	35.7
OM 91	Ra's Dibba monzogranitoids	1.43	7.26	0.119	0.512505 ± 6	−1.7	100.84	28.14	10.367	0.719590 ± 9	0.706334	27.5
OM 628		2.17	9.86	0.133	0.512575 ± 6	−0.5	13.16	189.79	0.201	0.706730 ± 9	0.706473	29.5
OM 124	Wadi Hulw bin Sulayman	5.80	19.55	0.180	0.512305 ± 6	−6.3	128.54	39.07	9.517	0.722223 ± 9	0.710054	80.4
OM 119	leucogranites	2.05	7.65	0.162	0.512313 ± 6	−6.0	129.22	56.16	6.657	0.718358 ± 10	0.709845	77.4
OM 118		4.92	19.93	0.149	0.512315 ± 6	−5.8	139.16	75.85	5.307	0.715961 ± 10	0.709175	67.9
OM 99	Wadi Zikt granites	1.83	7.84	0.141	0.512463 ± 6	−2.8	27.41	168.20	0.471	0.707367 ± 9	0.706764	33.6
Bani Hamid granulites												
OM 132	Alkali feldspar-phlogopite-diopside-	5.57	21.85	0.154	0.512702 ± 6	1.7	2.33	313.99	0.021	0.703959 ± 9	0.70392	−6.6
OM 135	-spinel granulite gneisses	2.33	6.29	0.224	0.512953 ± 6	5.8	6.24	119.04	0.152	0.705771 ± 8	0.705577	16.8
JC 92	Quartz-diopside-andradite gneiss	1.42	4.34	0.198	0.512315 ± 6	−6.3	0.17	5.60	0.089	0.709847 ± 18	0.709734	75.8
JC 94	Calc-silicate gneiss	1.88	9.54	0.119	0.512476 ± 5	−2.3	6.76	200.39	0.098	0.708143 ± 8	0.708018	51.4
JC 95	Quartz-phlogopite-cordierite gneiss	0.05	0.24	0.117	0.512256 ± 25	−6.5	0.98	3.66	0.773	0.709059 ± 11	0.7087071	52.2
Normal metamorphic sole, Sumeini												
OM 65	Garnet-diopside amphibolite gneiss	4.11	13.62	0.182	0.512862 ± 5	4.5	8.47	163.72	0.150	0.705608 ± 8	0.705417	14.5

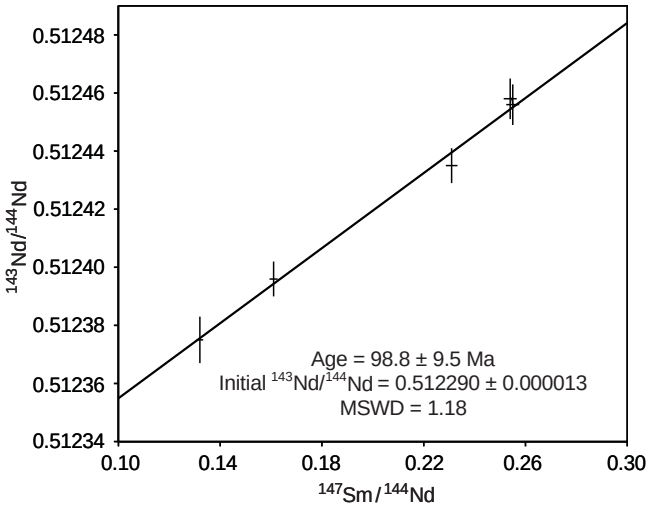

Fig. 9 Sm-Nd isochron for cogenetic analyses OM 79, OM 85, JC 25, JC 112 and OM 77 (Table 2), taken from a thick (~75 m) granitoid composite sill intruding mantle transition zone cumulate peridotites and gabbros sequence at Ra's Dadnah

Permo-Triassic to Jurassic tholeiitic to alkaline volcanics and associated volcanoclastic sediments found in the sub-ophiolitic Haybi complex (Searle 1980) and its subducted greenschist to granulite facies metamorphic equivalents, the Asimah and Bani Hamid metamorphic sole terrains. No Nd-Sr isotopic data are available for the volcanics of the Haybi complex, but Zeigler et al. (1991) present analyses of the Asimah tholeiitic and alkaline metavolcanic suite. New Rb-Sr and Sm-Nd analyses of granulite facies alkalic and tholeitic units from the Bani Hamid and Sumeini metamorphic sole localities are presented in Table 2. All Nd-Sr isotopic data relevant to the petrogenesis of the Khawr Fakkan block granitoids are presented in Fig. 10.

We propose that the LILE and volatile enriched mantle wedge above the intra-oceanic subduction zone that obducted the Semail ophiolite is preserved as the basal mantle sequence serpentinised harzburgites of the Khawr Fakkan block. Lanphere et al. (1981) and Zeigler et al. (1991) report basal mantle sequence harzburgite analyses that have positive ε_{Sr} values and differ greatly from the analyses reported by McCulloch et al. (1981). Chen and Pallister (1981) and Briqueu et al. (1991) have reported Pb isotopic data for Semail ophiolite mantle sequence harzburgites and the ophiolite metamorphic sole. Chen and Pallister (1981) analysed hydrothermal galena and serpentinised harzburgite from the basal mantle sequence in the Ibra area of the southern Oman mountains and concluded that both contained continentally derived Pb. Briqueu et al. (1991) demonstrated that these mantle sequence analyses had a similar Pb isotopic composition to granulite facies sedimentary material from the Bani Hamid terrain, and concluded that devolatilisation of the Bani Hamid granulites may have induced melting and metasomatism of the overlying mantle wedge. We propose that the LILE enrichment implicit in these analyses is attributable to the prograde devolatilisation of sediments subducted beneath the hot ophiolite or to contamination of the mantle wedge by ascending granitic melts. Fluids circulating at the base of the mantle wedge perhaps caused some or all of the widespread mantle sequence serpentinisation. Mixing calculations, using typical harzburgite compositions (1.1 ppm Sr, 0.035 ppm Nd, Lanphere et al. 1981; McCulloch et al. 1981) and the leucogranites of Wadi Hulw bin Sulayman as end members, however rule out the possibility of major

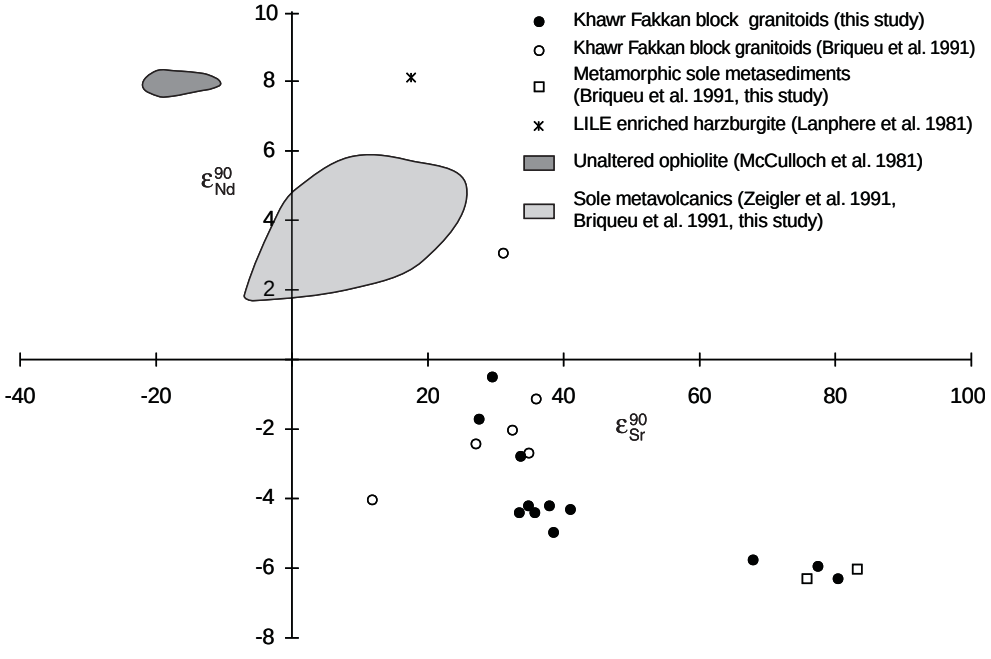

Fig. 10 ε_{Nd}–ε_{Sr} diagram showing the hyperbolic array defined by analyses of granitoid dykes from the Khawr Fakken block of the Semail ophiolite. Also shown for comparison are the potential mixing end members discussed in the text

mantle wedge mixing as a genetic mechanism. This mixing model requires granites formed by melting of the continental end member to have assimilated 100 times as much harzburgite to obtain the isotopic signature of the Ra's Dadnah composite dyke. This mechanism must therefore be discarded.

The metamorphic equivalents of the Haybi volcanics, represented by the Bani Hamid and Asimah terrain metavolcanics, have a wide range of ε_{Nd} and ε_{Sr} values. This may be expected from a diverse volcanic sequence, evolving compositionally over time, from a heterogeneous source (Searle 1980; Zeigler et al. 1991). All have lower ε_{Nd} values and higher ε_{Sr} values than the Semail ophiolite (Fig. 10). This suggests the subducted basaltic material was altered by interaction with seawater. McCulloch et al. (1981) estimated seawater locally to have had an ε_{Sr} value of $\sim$30. The LILE enriched, subducted metabasalts have values approaching this figure. Mixing calculations using such a subducted metabasalt suggest the Ra's Dibba monzogranitoids contain $\sim$65% of the basaltic end member, components of the Ra's Dadnah composite dyke between 30 and 50%, and the Wadi Hulw bin Sulayman dykes less than 5%.

We propose that the observed hyperbolic trend of granitoid intrusions analysed in this study can be accounted for by mixing between the immediate precursors of the Wadi Hulw bin Sulayman peraluminous leucogranitoids (the quartzofeldspathic components of the Bani Hamid metamorphic terrain) and LILE enriched, metabasaltic extrusives or derived arc sediments subducted beneath the ophiolite. These units are preserved unmetamorphosed in the Haybi complex and at greenschist (Asimah) and granulite (Bani Hamid) facies in the metamorphic sole. The basaltic metamorphic sole end member component used in mixing calculations has the composition: 200 ppm Sr, 7 ppm Nd, $^{147}Sm/^{144}Nd = 0.194$, $\varepsilon_{Nd} = 5.05$, $\varepsilon_{Sr} = 26$ (Zeigler et al. 1991).

Sm-Nd isotope systematics

Mixing relationships between the two chosen end members are shown in Fig. 11. The curvature of the mixing line in Fig. 11 is controlled only by the Nd/Sr ratios of the end members. It matches the observed hyperbolic array of the analysed granitoids well, suggesting that mixing between LILE enriched metabasaltic material and Bani Hamid granulite derived melts can explain the observed hyperbolic array. However, Sm-Nd isotope systematics indicate that the source relationships may be more complex since there is a considerable spread of data on a Sm-Nd isochron diagram (Fig. 12). For example, the granites may have formed by the mixing of melts derived from two contrasting subducted components, or from mixed sedimentary material (quartzofeldspathic and volcanoclastic). In the latter case, the observed two component mixing would have a pre-magmatic source.

Pure mixing components should lie on a straight line between the mantle and metasedimentary sources on Fig. 12 and, although individual dyke domains do define linear trends, they do not lie on the modelled mixing line. However, a linear array would only be expected if the granitoid melts had assimilated mantle material or mixed with such melts. If the mixing was pre-magmatic, any linear relationship between the melts and the source components would be altered by subsequent anatexis and fractional crystallisation. Partial melts from such a

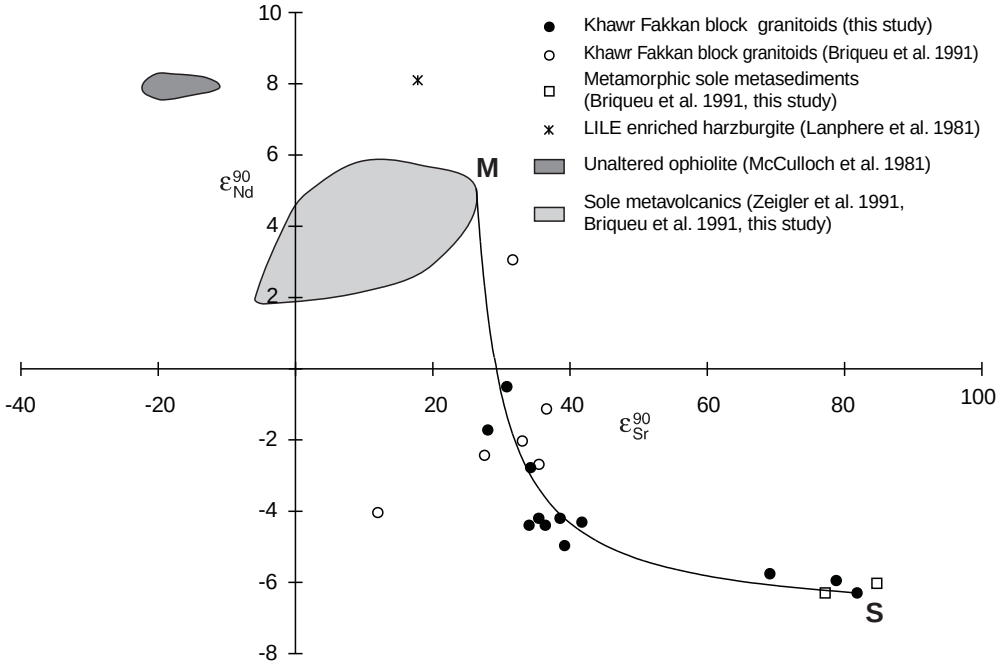

Fig. 11 ε_{Nd} versus ε_{Sr} diagram in which the array defined by the granitoid dykes is compared with calculated two component mixing. The assumed end member compositions are represented by an alkali metabasalt from the metamorphic sole (*M*) and a metasedimentary component (Wadi Hulw bin Sulayman leucogranite, *S*). The *curvature* of the mixing line is controlled only by the Nd/Sr ratios of the two end members. Using values from Table 3 for *S* and Zeigler et al. (1991) for *M* gives a good fit to the granitoid dyke array and suggests they may have formed by mixing between these two contrasting sources

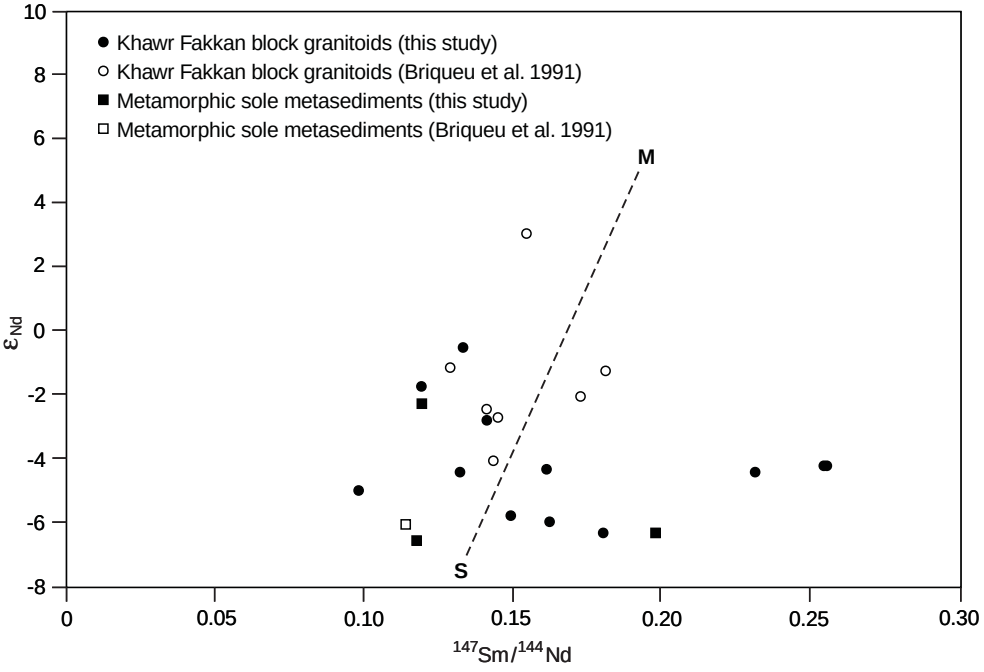

Fig. 12 ε_{Nd} versus $^{147}Sm/^{144}Nd$ isochron diagram that shows Sm-Nd isotope systematics of the granitoid dyke suite and its contrasting hypothetical source components. The *broken line* represents pure mixing between the Bani Hamid metasediments (*S*, $^{147}Sm/^{144}Nd = 0.12$ and $\varepsilon_{Nd} = -6.0$) and the metabasaltic sole components (*M*, $^{147}Sm/^{144}Nd = 0.19$ and $\varepsilon_{Nd} = 5.05$, data from Zeigler et al. 1991). Source contamination of the sedimentary melts is implied because the individual dyke suite trends do not converge at the sedimentary component data point. See text for discussion. Data symbols as Fig. 10

source should plot at lower Sm/Nd ratios with the degree of displacement from the mixing line dependent on the degree of melting and source partition coefficients. These initial compositions could subsequently be modified by fractional crystallisation processes, which would produce arrays with variable Sm/Nd ratios but near constant ε_{Nd}. There is abundant field evidence of fractional crystallisation processes. The Wadi Hulw bin Sulayman leucogranites may have formed by the fractional crystallisation of alkali feldspar from a minimum melt derived directly from the quartzofeldspathic granulites of the Bani Hamid terrain. The fact that the continental end member on Fig. 11 is not intersected by the granitoid trends on Fig. 12 is consistent with source mixing (Pedersen and Dunning 1997).

Discussion

Leucocratic trondhjemites comprise $\ll 0.5\%$ of the Semail ophiolite sequence and represent the products of extreme fractionation of a basaltic parent magma (Lippard et al. 1986). They consist mainly of plagioclase and quartz with minimal K_2O or mafic minerals (Pedersen and Malpas 1984). Leucogranitic material, such as that seen in the Khawr Fakkan block of the Semail ophiolite, has not been commonly reported from ophiolitic terrains. The distinction, in terms of geochemistry, mineralogy and structural position, between the analysed dyke suite and the trondhjemites of the ophiolite late intrusive sequence is clear. They are also distinct from the rare tonalitic partial melt pods observed within amphibolite to granulite facies metabasalts of the ophiolite metamorphic sole.

Barbarin (1996) recognised two contrasting types of peraluminous anatectic melts: minimum melt leucogranitoids, characterised by the presence of primary muscovite, and biotite rich monzogranitoids, characterised by the presence of cordierite and accessory aluminium silicates. The characteristic phases of such melts may be related by the equation:

$$Kfs + Grt + Crd + H_2O = Ms + Bt + Qtz$$

The inference that high water activity favours the production of muscovite bearing granitoids leads to the conclusion that such granitoid parageneses are characteristic of highly tectonised zones. Shearing in such zones facilitates partial melting (by the provision of fluid channels) and produces often deformed and pegmatitic muscovite bearing melts that have low vertical mobility and remain close to their sources, a situation well seen in the deformed leucogranitoids of Wadi Hulw bin Sulayman. In contrast, cordierite bearing granitoids can be produced without the addition of externally derived H_2O in less deformed tectonic environments such as at Ra's Dibba. These contrasting examples demonstrate that variations in the physical conditions of partial melting, as well as source heterogenity, can control the mineralogy and tectonic distribution of granitoid melts.

A complementary petrogenetic scheme for collisional granitoids, proposed by Harris et al. (1986) differentiates between muscovite bearing, syn-collisional leucogranitoids produced directly by the anatexis of metasediments, as in Wadi Hulw bin Sulayman, and post-collisional granitoids, formed from LILE enriched mantle melts, and characterised by the presence of magmatic cordierite with enclaves and xenoliths of mafic material, as at Ra's Dibba.

Age of the dyke suite

No U-Pb (crystallisation) ages have been determined for the Khawr Fakkan block granitoids (Alleman and Peters 1972; Gnos and Peters 1993; Hacker et al. 1996). Published ages of granitoid material within the Semail ophiolite are restricted to the K-Ar and Ar-Ar systems, and plagiogranitic and leucogranitic granitoid parageneses are not clearly distinguished. Muscovite $^{40}Ar/^{39}Ar$ cooling ages from garnet bearing granitoid dykes in the Khawr Fakkan block average 89.5 ± 0.4 Ma (Hacker et al. 1996), and ages of Khawr Fakkan block peraluminous granitoids from Gnos and Peters (1993) average 90.4 ± 0.9 Ma. These are cooling ages. The Sm-Nd isochron age of 98.8 ± 9.5 Ma presented in Fig. 9 is indistinguishable from the accepted mean crystallisation age (94.8 ± 0.1 Ma) of the ophiolite crustal sequence (Tilton et al. 1981). The formation of residual harzburgite from the melting event that produced the ophiolite crustal sequence has been estimated to predate crystallisation of the crustal sequence by at most 6 Ma (McCulloch et al. 1981). Structural evidence suggests that the crystallisation of the Ra's Dadnah composite granitoid sill postdated the formation of the residual harzburgites of the ophiolite mantle sequence, and must therefore be younger than ~101 Ma. The peak metamorphism of the Bani Hamid terrain at ~95 Ma (Hacker et al. 1996) is also truncated by and therefore older than the granitoid dyke suite. The K-Ar granitoid cooling ages which, in conjunction with ophiolite cooling rates (~200 °C Ma^{-1} between 94.8 Ma and 93.5 Ma; Hacker et al. 1996) and metamorphic sole (~90 °C Ma^{-1} between 93.5 Ma and 92.6 Ma and ~20 °C Ma^{-1} until biotite closure at 89.2 Ma; Hacker et al. 1996) cooling rates can be used to estimate a crystallisation age of ~93 Ma for the dykes, assuming a solidus temperature of ~650 °C at 2.5 kbar for the dykes (Peters and Kamber 1994) and a muscovite closure temperature in the K-Ar system of ~475 °C (Hacker et al. 1996). The granitoid dykes were clearly associated with the initial stages of sub-ophiolite metamorphism and ophiolite obduction. The age of the greenschist facies metamorphism of some dykes, if correlated with the similar grade overprint event observed in the adjacent Bani Hamid and normal metamorphic sole sequences, can provide a *minimum* emplacement age. Gnos and Peters (1993) dated an actinolitic rim of pargasitic hornblende from a Bani Hamid sequence hornblende granulite at 91.2 ± 0.5 Ma (K-Ar).

Tectonic model

The granitoid dykes of the northern Semail ophiolite present a number of unique petrogenetic features. The proposed model (Fig. 13) is consistent with the observed

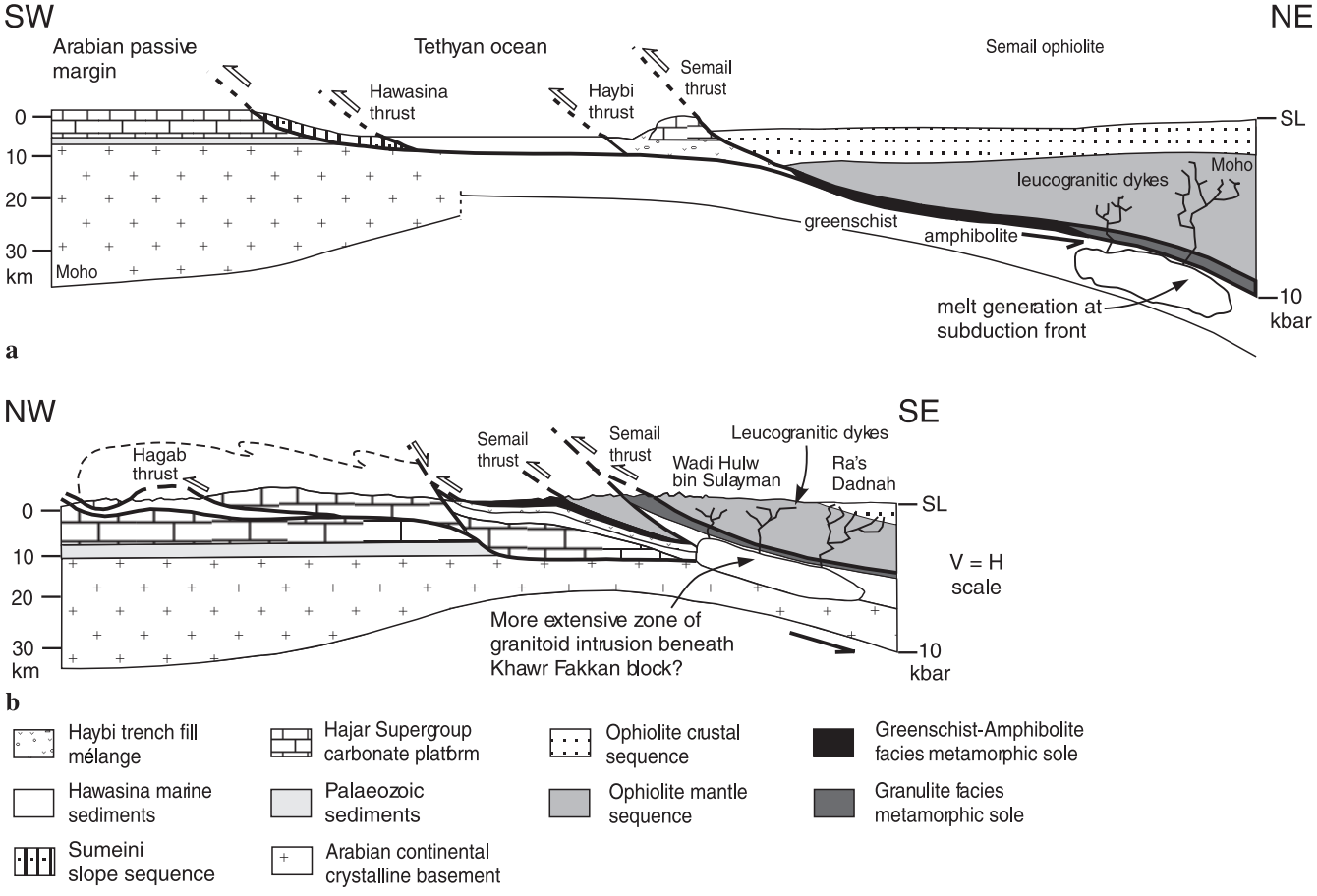

distribution of granitoid dykes. The most "continental" leucogranitic melts (Wadi Hulw bin Sulayman) occur adjacent to their metasedimentary source, the Bani Hamid granulites, at the deepest structural levels within the ophiolite, and hybrid melts are observed at higher structural levels (Ra's Dadnah). The enrichment of the mantle wedge above the subduction zone by LILE enriched volatiles, derived from subducted oceanic crust, may explain in part the peralkaline nature of some of the dykes intruded at higher structural levels. The presence of minimum melt type leucogranites in heavily sheared ophiolite domains (Wadi Hulw bin Sulayman is adjacent to the Semail thrust at the base of the ophiolite) follows the prediction of Barbarin (1996), and also accounts for the presence of these low mobility melts close to their source. In contrast, higher structural levels (Ra's Dibba) are occupied by biotite-cordierite monzogranitoids resulting from the partial melting of hybrid metasedimentary and oceanic crustal source components.

Eclogite barometry in the As Sifah region of the southern Oman mountains (Fig. 1) has demonstrated the subduction of the Arabian continental passive margin to depths of ~80 km beneath the Semail ophiolite (Searle et al. 1994). The exact timing of this H*P* event is the major unresolved issue in the obduction and emplacement history of the Semail ophiolite. The As Sifah eclogites muscovite $^{40}Ar/^{39}Ar$ plateau age is 96 ± 2 Ma (Searle et al. 1994), similar to the mean $^{40}Ar/^{39}Ar$ age of 93.5 ± 0.1 Ma for sole metamorphism in the adjacent Wadi Tayin area (Hacker et al. 1996). This suggests that the H*P* metamorphism was roughly contemporaneous with the formation of the ophiolite and the metamorphic sole, rather than at ~80 Ma as suggested by Michard et al. (1994). In the northern mountains, the mean age of sole metamorphism is 94.9 ± 0.2 Ma (Hacker et al. 1996). Here, intra-oceanic subduction resulted in higher temperatures and lower pressures of metamorphism, and the generation of granitoid melts whereas, to the south, the subduction of a continental promontory (Searle et al. 1994; Hacker and Gnos 1997) led to higher pressures and lower temperatures of metamorphism.

The H*P* and H*T* terrains both exhibit a greenschist facies overprint, which has been dated as 91.2 ± 0.5 Ma (Gnos and Peters 1993) in the Bani Hamid terrain, and a *maximum* of 93.7 ± 0.8 Ma in the Wadi Tayin area (Hacker et al. 1996). No age estimates exist for the greenschist facies overprint in the As Sifah area. If these overprints all belong to the same (regional) metamorphic event, then the subducted continental margin, the metamorphic sole and the anatectic granitoids were all at a similar crustal level, at a depth of ~10–15 km, by ~91 Ma. We propose that the available geochronological evidence is most compatible with the fact that the separate H*T* and H*P* metamorphic events were contemporaneous at around 95 Ma. The limited contemporary surface expression of the contrasting terrains along the Oman mountains belt may be related in part to Tertiary deformational events such as the formation of the Musandam culmination and the doming of the Saih Hatat window.

The temporal relationship between the formation of the eclogite facies material and the ophiolite metamorphic sole in the As Sifah/Wadi Tayin area is the key to understanding the plate configuration during the obduction process. The eclogites reached a peak temperature of 540 ± 75 °C (Searle et al. 1994), similar to temperatures in the metamorphic sole at ~94 Ma (Hacker and Gnos 1997); it is unlikely that they formed at the same time in a single subduction zone. The tectonic model of Searle et al. (1994) is compatible with all the available structural and geochronological evidence and favours the presence of twin subduction zones. The eclogites formed in a subduction zone close to the Arabian continental margin, with the metamorphic sole and related anatectic granitoids forming in an intra-oceanic subduction zone further outboard.

◄

Fig. 13a, b Tectonic model for the generation and emplacement evolution of the Khawr Fakkan block leucogranitoid dykes. **a** Shows the proto-ophiolite above a NE dipping subduction zone within Tethys, during the Cenomanian (~95 Ma). Initiation of intra-oceanic subduction at ~105–100 Ma (Lippard et al. 1986) and movement along the Semail thrust was followed by the initiation of spreading and the crystallisation of the plagiogranitic components of the ophiolite crustal sequence. The Arabian continental margin thinned towards the NE, and the crust beneath the Hawasina pelagic basin and Haybi trench fill units consisted of attenuated transitional crust containing alkalic ultramafic and basaltic intrusions of Triassic and Jurassic age. Subduction of this oceanic crust and its sediment cover, represented by the trench fill components of the Haybi complex (Searle 1980), including Permo-Triassic seamounts and the pelagic marine sediments of the Hawasina basin, led to anatexis by the dehydration melting of muscovite rich sedimentary material at 650–700 °C (Peters and Kamber 1994) and 3–5 kbar at the subduction front. Minimum melt type granitoids produced in this manner were hybrid melts, containing variable proportions of continental and mantle components and several distinct suites were emplaced up to the base of the ophiolite crustal sequence. The Bani Hamid granulite facies terrain records peak conditions of >800 °C and <10 kbar (Gnos and Kurz 1994) driven by the residual heat of the overlying mantle wedge. **b** Present day section through the Khawr Fakkan block of the Semail ophiolite in the UAE. SW propagated thrusting of the ophiolite and its metamorphic sole, accompanied by up to 400–500 km shortening within the pelagic (Hawasina), carbonate slope (Sumeini) and shelf sequences of the passive margin, led to the emplacement of the cool ophiolite onto the Arabian continental margin by ~78 Ma (Hacker et al. 1996). Subsequent Tertiary thrusting (the Hagab thrust) produced the Musandam culmination and may have initiated the out of sequence thrusting that repeated the ophiolite mantle sequence and exhumed the Bani Hamid granulite facies metamorphic sheet. The presence of a more extensive zone of peraluminous granitoid intrusion at depth within the mantle sequence of the Khawr Fakkan block of the ophiolite, below present erosion levels, is possible as in the Caledonian Karmoy ophiolite of SW Norway (Pedersen and Dunning 1997)

Concluding remarks

1. Major and trace element analyses demonstrate that the leucogranitic dykes of the Khawr Fakkan block of the Semail ophiolite are compositionally similar to crustal melt leucogranites from the Himalaya and other collisional environments.

2. The CIPW normative ternary system diagrams indicate that the granitoid melts found at the lowest structural levels exhibit minimum melt type compositions and were formed by the dehydration melting of muscovite bearing sediments at 3–5 kbar. Melts emplaced at higher structural levels formed by H_2O saturated melting.

3. The LILE (Sr, Rb and Ba) covariation modelling shows that the structurally lowest granitoids formed by the dehydration melting of the Bani Hamid granulite metasediments. Melts emplaced at higher structural levels underwent a greater degree of partial melting (e.g. Ra's Dadnah) forming diverse but cogenetic suites (ranging from peraluminous hornblende-biotite diorites to garnet-tourmaline leucogranites) due to the fractional crystallisation of alkali feldspar and biotite.

4. A new Sm-Nd isochron from the Ra's Dadnah composite dyke gives an age of 98.8 ± 9.5 Ma. Structural considerations, published granitoid K-Ar and $^{40}Ar/^{39}Ar$ cooling ages and existing ophiolite age constraints indicate that the dyke suite is younger than ~95 Ma and older than ~91 Ma.

5. The analysed dykes formed by the melting of trench fill Haybi complex material (subsequently metamorphosed to granulite facies) at the subduction front beneath the ophiolite. The Sr-Nd isotope systematics show that the observed two component mixing reflects pre-magmatic mixing between contrasting quartzofeldspathic and basaltic components. The latter source may represent volcanoclastic sediments derived from volcanic islands on the subducting continental margin.

6. The absence of significant Rb-Sr isotopic disequilibrium between the granitoid dyke suite and the subducted source sediments, despite assumed rapid advective heating of the sediments subducted beneath the hot ophiolite, may be due to subduction zone isotopic homogenisation during melt extraction. Dynamic recrystallisation due to shearing in the subduction zone would have facilitated this process.

It is possible that the granitoid dyke suite represents the highest structural levels of a more extensive zone of granitoid intrusion at the base of the ophiolite mantle sequence, as in the Karmoy ophiolite of SW Norway (Pedersen and Dunning 1997). The unique status of the Semail ophiolite as an exposed example of SSZ mantle, and the study of the petrogenetic and metamorphic processes related to the generation and emplacement of the ophiolite, may have parallels with processes in similar intra-oceanic arcs observable today.

Further work on the Sr and Nd isotope systematics of the units of the Haybi trench mélange sediments and their granulite facies equivalents in the ophiolite metamorphic sole will enable the relationships between the postulated sources and the studied granites to be understood more fully. Accurate U/Pb dating of the granitic material in the Khawr Fakkan block of the ophiolite would constrain subduction zone processes and rates in the intra-oceanic arc environment where the ophiolite formed. The recognition of similar leucogranitic dykes within the ophiolite mantle sequence in the southern mountains will help to further constrain existing tectonic models of the obduction and emplacement history of the Semail ophiolite and the relationships between the contrasting types of subduction-obduction related ophiolite metamorphism seen in the Oman mountains.

Acknowledgements This work was funded by a NERC PhD grant (GT4/96/226/E) to J.C. and a NERC grant (GT5/96/13/E) to M.S.. Thanks to Tjerk Peters for suggesting granite localites and sharing his UAE granite collection, Hilal bin Mohd. Al Azri (Directorate General of Petroleum and Minerals, Ministry of Commerce and Industry, Muscat) for sponsorship, and the Willis family in Muscat. The isotopic and geochemical analyses were conducted at Bergen University, Norway: the first author would like to thank the staff of the Geology department for their patient laboratory assistance. Thanks to Edwin Gnos, Louis Briqueu, Julian Pearce and Brad Hacker for reviews.

References

Alabaster T, Pearce JA, Malpas J (1982) The volcanic stratigraphy of the Oman ophiolite complex. Contrib Mineral Petrol 81: 168–183

Allemann F, Peters Tj (1972) The ophiolite-radiolarite belt in the north Oman mountains. Eclogae Geol Helv 65: 657–697

Barbarin B (1996) Genesis of the two main types of peraluminous granitoids. Geology 24: 295–298

Barker F (1979) Trondhjemite: definition, environment and hypotheses of origin. In: Barker F (ed) Trondhjemites, dacites and related rocks. Elsevier, Amsterdam, pp 1–12

Bechennec F, LeMetour J, Rabu D, Villey M, Beurrier M (1988) The Hawasina basin: a fragment of a starved passive continental margin, thrust over the Arabian platform during obduction of the Semail nappe. Tectonophysics 151: 323–343

Boudier F, Bouchez JL, Nicolas A, Cannat M, et al (1985) Kinematics of oceanic thrusting in the Oman Ophiolite: model for plate convergence. Earth Planet Sci Lett 75: 215–222

Boudier F, Ceuleneer G, Nicolas A (1988) Shear zones, thrusts and related magmatism in the Oman ophiolite: initiation of thrusting at an oceanic ridge. Tectonophysics 151: 275–96

Briqueu L, Mevel C, Boudier F (1991) Sr, Nd and Pb isotopic constraints in the genesis of a calc-alkaline plutonic suite in the Oman ophiolite related to the obduction process. In: Peters Tj, Nicolas A, Coleman RG (eds) Ophiolite genesis and evolution of the oceanic lithosphere. Kluwer, The Netherlands, pp 517–42

Browning P (1982) The petrology, geochemistry and structure of the plutonic rocks of the Semail ophiolite (unpublished). Phd thesis, Open Univ, Milton Keynes

Bucher M, Kurz D (1991) The metamorphic series associated with the Oman ophiolite nappe of the Oman mountains in the United Arab Emirates. MSc thesis, Univ Bern

Chappell BW, White AJR (1992) I and S type granites in the Lachlan Fold Belt. Trans R Soc Edinburgh Earth Sci 83: 1–26

Chen JH, Pallister JS (1981) Lead isotopic studies of the Semail ophiolite, Oman. J Geophys Res 86: 2699–2706

Coleman RG (1981) Tectonic setting for ophiolite obduction in Oman. J Geophys Res 86: 2497–2508

Coleman RG, Hopson CA (1981) (eds.) Oman ophiolite special issue. J Geophys Res 86

DePaolo DJ, Wasserburg GJ (1976a) Nd isotopic variations and petrogenetic models. Geophys Res Lett 3: 743–746

DePaolo DJ, Wasserburg GJ (1976b) Inferences about magma sources and mantle structure from variations in $^{143}Nd/^{144}Nd$. Geophys Res Lett 4: 465–468

Ghent ED, Stout MZ (1981) Metamorphism at the base of the Semail Ophiolite. J Geophys Res 86: 2557–2571

Glennie KW, Boeuf MG, Hughes-Clarke MHW, Moody-Stuart M, et al (1974) Geology of the Oman mountains. Verh K Ned Geol Mijnbouwk Genoot 31

Gnos E (1992) The metamorphic rocks associated with the Oman Ophiolite (Sultanate of Oman and United Arab Emirates) (unpublished). PhD thesis, Univ Bern

Gnos E (1998) Peak metamorphic conditions of garnet amphibolites beneath the Semail ophiolite: implications for an inverted pressure gradient. Int Geol Rev 40: 281–304

Gnos E, Kurz D (1994) Sapphirine-quartz and sapphirine-corundum assemblages in metamorphic rocks associated with the Semail ophiolite (United Arab Emirates). Contrib Mineral Petrol 116: 398–410

Gnos E, Nicolas A (1996) Structural evolution of the northern end of the Oman ophiolite and enclosed granulites. Tectonophysics 254: 111–37

Gnos E, Peters Tj (1993) K-Ar ages of the metamorphic sole of the Semail ophiolite: implications for ophiolite cooling history. Contrib Mineral Petrol 113: 325–332

Hacker BR (1994) Rapid emplacement of young oceanic lithosphere: argon geochronology of the Oman ophiolite. Science 265: 1563–65

Hacker BR, Gnos E (1997) The conundrum of Semail: explaining the metamorphic history. Tectonophysics 279: 215–226

Hacker BR, Mosenfelder JL (1996) Metamorphism and deformation along the emplacement thrust of the Semail ophiolite, Oman. Earth Planet Sci Lett 144: 435–51

Hacker BR, Mosenfelder JL, Gnos E (1996) Rapid emplacement of the Oman ophiolite: thermal and geochronological constraints. Tectonics 15: 1230–47

Harris NBW, Ayres M (1998) The implications of Sr isotope disequilibrium for rates of prograde metamorphism and melt extraction in anatectic terrains. In: Treloar PJ, O'Brien PJ (eds) What drives metamorphism and metamorphic reactions? Geol Soc London Spec Publ 138, pp 171–182

Harris NBW, Pearce JA, Tindle AG (1986) Geochemical characteristics of collision zone magmatism. In: Coward MP, Ries AC (eds) Collision tectonics. Geol Soc London Spec Publ 19, pp 185–201

Holtz F, Barbey P (1991) Genesis of peraluminous granites. 2. Mineralogy and chemistry of the Tourem Complex (north Portugal): sequential melting versus restite unmixing. J Petrol 32: 959–978

Inger S, Harris NBW (1993) Geochemical constraints on leucogranite magmatism in the Langtang valley, Nepal Himalaya. J Petrol 34: 345–368

Jacobsen SB, Wasserburg GJ (1984) Sm-Nd evolution of chondrites and achondrites. Earth Planet Sci Lett 67: 137–150

Lanphere MA (1981) K-Ar ages of metamorphic rocks at the base of the Semail Ophiolite, Oman. J Geophys Res 86: 2777–2782

Lanphere MA, Coleman RG, Hopson CA (1981) Sr isotopic tracer study of the Semail ophiolite, Oman. J Geophys Res 86: 2709–2720

LeFort P, Cuney M, Deniel C, France-Lanord C, et al (1987) Crustal generation of the Himalayan leucogranites. J Geophys Res B11: 10545–10568

Lippard SJ, Shelton AW, Gass IG (1986) The ophiolite of Northern Oman. Blackwell Scientific Publications, Oxford

McCulloch MT, Gregory RT, Wasserburg GJ, Taylor HP (1981) Sm-Nd, Rb-Sr and ^{18}O-^{16}O isotropic systematics in an oceanic crustal section; evidence from the Semail ophiolite. J Geophys Res 86: 2721–2735.

Michard A, Goffé B, Saddiqi O, Oberhänsli R, Wendt AS (1994) Late Cretaceous exhumation of the Oman blueschists and eclogites: a two stage extensional mechanism. Terra Nova 6: 39–49

Miller CF (1985) Are strongly peraluminous magmas derived from pelitic sedimentary sources? J Geol 93: 673–689

Montigny R, Le Mer O, Thuziat R, Whitechurch H (1988) K-Ar and $^{40}Ar/^{39}Ar$ study of the metamorphic rocks associated with the Oman ophiolite. Tectonophysics 151: 345–362

Nicolas A (1989) Structures of ophiolites and dynamics of oceanic lithosphere. Kluwer, The Netherlands

Patiño Douce AE, Harris NBW (1998) Experimental constraints on Himalayan anatexis. J Petrol 39: 689–710

Pearce JA (1989) High P/T metamorphism and granite genesis beneath ophiolite thrust sheets. Ofioliti 14: 195–211

Pearce JA, Alabaster T, Shelton AW, Searle MP (1981) The Oman ophiolite as a Cretaceous arc-basin complex: evidence and implications. Philos Trans R Soc London A300: 299–317

Pearce JA, Harris NBW, Tindle AG (1984) Trace element discrimination diagrams for the tectonic interpretation of granitic rocks. J Petrol 25: 956–983

Pedersen RB, Dunning GR (1997) Evolution of arc crust and relations between contrasting sources: U-Pb (age), Nd and Sr isotope systematics of the ophiolitic terrain of SW Norway. Contrib Mineral Petrol 128: 1–15

Pedersen RB, Malpas J (1984) The origin of oceanic plagiogranites from the Karmoy ophiolite, Western Norway. Contrib Mineral Petrol 88: 36–52

Peters Tj, Kamber BS (1994) Peraluminous, potassium-rich granitoids in the Semail Ophiolite. Contrib Mineral Petrol 118: 229–38

Pin C, Briot D, Bassin C, Poitrasson F (1994) Concomitant separation of strontium and samarium-neodymium for isotope analyses in silicate samples, based on specific extraction chromatography. Anal Chim Acta 298: 209–217

Potts PJ (1987) A handbook of silicate rock analysis. Blackie Academic and Professional, London

Richard P, Shimizu N, Allégre CJ (1976) $^{143}Nd/^{146}Nd$, a natural tracer: an application to oceanic basalts. Earth Planet Sci Lett 31: 269–278

Rollinson HR (1993) Using geochemical data: evaluation, presentation, interpretation. Longman Scientific and Technical, London

Searle MP (1980) The metamorphic sheet and underlying volcanic rocks beneath the Oman ophiolite in the northern Oman mountains of Arabia (unpublished). PhD thesis, Open Univ, Milton Keynes

Searle MP (1984) Alkaline peridotite, pyroxenite and gabbroic intrusions in the Oman mountains, Arabia. Can J Earth Sci 21: 396–406

Searle MP, Cox JS (1999) Tectonic setting, origin and obduction of the Oman Ophiolite. Bull Geol Soc Am 111: 104–122

Searle MP, Fryer BJ (1986) Garnet, tourmaline and muscovite bearing leucogranites, gneisses and migmatites of the Higher Himalaya from Zanskar, Kulu, Lahoul and Kashmir. In: Coward MP, Ries AC (eds) Collision tectonics. Geol Soc London Spec Publ 19, pp 185–201

Searle MP, Malpas J (1980) The structure and metamorphism of rocks beneath the Semail Ophiolite of Oman and their significance in ophiolite obduction. Trans R Soc Edinburgh Earth Sci 71: 247–262

Searle MP, Malpas J (1982) Petrochemistry and origin of sub-ophiolite metamorphic and related rocks in the Oman Mountains. J Geol Soc London 139: 235–248

Searle MP, Waters DJ, Martin HN, Rex DC (1994) Structure and metamorphism of blueschist-eclogite facies rocks from the northeastern Oman mountains. J Geol Soc London 151: 555–576

Steiger RH, Jager E (1977) Submission on geochronology: convention on the use of decay constants in geo- and cosmochronology. Earth Planet Sci Lett 36: 359–362

Tilton GR, Hopson CA, Wright JE (1981) Uranium-lead isotopic ages of the Semail ophiolite, Oman with application to Tethyan ocean ridge tectonics. J Geophys Res 86: 2763–2775

Tippit PR, Pessagno EA, Smewing JD (1981) The biostratigraphy of sediments in the volcanic unit of the Semail Ophiolite. J Geophys Res 86: 2756–2762

Zeigler URF, Stoessel GFU, Peters Tj (1991) Isotopic (Rb-Sr and Sm-Nd) and geochemical studies of the metamorphosed volcanic rocks in the metamorphic series below the Semail ophiolite in the Dibba zone (United Arab Emirates). Schweiz Mineral Petrogr Mitt 71: 19–33